

対流性降雨の発生に及ぼす都市の影響に関する研究 (英文)

著者	米谷 恒春
雑誌名	国立防災科学技術センター 研究報告
巻	44
ページ	1-59
発行年	1989-01
URL	http://doi.org/10.24732/nied.00000993

Study of the Urban Effects on the Occurrence of Convective Precipitation*

By

Tsuneharu Yonetani

National Research Center for Disaster Prevention, Japan

Abstract

The effects that urban environments have on the occurrence of convective precipitation are studied from three different approaches: theoretical, case studies, and statistical analysis. The results show that a heat island in an urban area has a marked influence on the development of a convective phenomenon with precipitation.

Numerical experiments show the following: (1) a heat island modifies the atmosphere so that convective clouds may develop well over it and the heat island can form a cloud which in turn causes rain; (2) the formation and the development of a cloud are so directly affected by conditions of a lower air layer modified by the heat island that convective clouds which are formed over heat islands with various horizontal scales behave differently; (3) when the size of the heat island is comparable to the size of an urban area, it causes cumulus convection to be most active.

It is the upward motion in the lower layer and not destabilization of static stability that directly enhances the convective activity over the heat island. The horizontal motion accompanied with the upward motion decreases temperature and the decrease of temperature becomes larger as the heat island is smaller. Conversely, when the heat island is larger, the upward motion is slight. These conditions are unfavorable for the development of cumulus convection. This is why heat islands of a suitable size enhance cumulus convection most as described in item (3) above.

Next, three cases which show unusually large amounts of rainfall recorded in the Tokyo urban area are examined.

The analysis of radar echoes suggests that the occurrence of heavy rainfall was affected by the heat island. Two echoes first appeared over the noticeable heat island and rapidly expanded. There was another rapid expansion of an echo over the heat island. These three echoes combined and formed a large echo, which covered the northern part of the highly developed Tokyo area. In this way, echoes developed and caused heavy localized rainfall.

After that, the large echo moved southward and a part of the echo passed over another heat island. Heavy rainfall occurred in and around the heat island again.

* Doctor thesis submitted to Tsukuba University

These situations are similar to what the numerical simulation shows.

In the other two case studies, there was a noticeable heat island in which the convergence of surface air occurred about an hour prior to the occurrence of heavy rainfall. Rainfall was especially heavy in and around the heat island when a general wind was weak.

Finally, a statistical analysis reveals the magnitude of the effect of the heat island on convective precipitation. An analysis of daily precipitation in August shows a trend for the highly developed Tokyo area to have heavy precipitation more often than at any other time. A close relationship exists between the frequencies of appearances of heavy precipitation and a sizable heat island in this area. This coincidence suggests that the heat island is a predominant causative factor in the occurrence of heavy precipitation in the highly developed Tokyo area.

Conditions favorable to the occurrence of strong precipitation in the highly developed Tokyo area are also statistically analyzed. The average daily relative humidity is 84% on days with strong precipitation in the highly developed area, while it is 74% on days with strong precipitation in the surroundings. This means that a heat island is less capable of producing strong convective precipitation than other mechanisms which cause this type of precipitation in the surroundings.

The following features are also shown : within six days with strong precipitation in the surroundings, with a mean relative humidity of not less than 80%, a sizable heat island was present for four of the days in the highly developed area ; there were 11 days with strong precipitation in this area and each day experienced a noticeable heat island . The number of days with strong precipitation is larger in the highly developed area than in the surroundings despite the fact that the total monthly precipitation is smaller in the developed area. These findings suggest that a heat island can cause convective precipitation more efficiently than any other mechanism which produces convective precipitation when the atmospheric conditions are favorable.

The following conclusion is drawn : A sizable heat island in an urban area is less capable of producing convective precipitation than other mechanisms which cause it, but the heat island can be an important causative factor in the occurrence of convective precipitation including heavy localized rainfall, especially in humid areas. This is because the heat island induces an upward motion of air over the area. The upward motion can be a trigger force for the occurrence of a convective storm and can enhance convective activity by increasing the amount of water vapour supplied to a convective storm.

Kew word : Urban climatology, heavy precipitation

CONTENTS

	Page
LIST OF SYMBOLS	3
1. INTRODUCTION	4
1-1 Background and Purpose of the Study	4
1-2 Review of Previous Studies	5
2. THEORETICAL STUDY	8
2-1 Numerical Experiment	8
2-2 Analysis of the Effects of the Heat Island on the Development of a Cloud	19
2-3 Discussion	21
3. CASE STUDIES	22
3-1 Data Used and Definition of Areas	22
3-2 The Case of 22 July, 1981	23
3-3 The Case of 14 July, 1985	28
3-4 The Case of 15 May, 1979	32
3-5 Discussion	35
4. STATISTICAL STUDY	37
4-1 Increase in Number of Days with Heavy Precipitation in Tokyo Built-up Area	37
4-2 Possibility for the Heat Island to Affect on Precipitation	43
4-3 Discussion	46
5. CONCLUSIONS	48
ACKNOWLEDGMENTS	49
APPENDIX A	50
APPENDIX B	52
REFERENCES	53

LIST OF SYMBOLS

c_p	specific heat of air at constant pressure
D_f	diffusion term of a variable f
F_r	radial component of frictional force
F_z	vertical component of frictional force
g	acceleration of gravity
K	total kinetic energy
L_e	latent heat of condensation
P	pressure
P_c	rate of production of cloud water
P_e	rate of evaporation of liquid water
P_r	rate of production of rain water
Q_c	mixing ratio of cloud water
Q_l	mixing ratio of liquid water
Q_r	mixing ratio of rain water
Q_t	mixing ratio of total water
Q_v	mixing ratio of water vapour
q_s	saturation mixing ratio of water vapour

R_L	radius of integration domain
R_v	gas constant of water vapour
r	radial coordinate
r_h	radius of heat island
T	temperature
T_v	virtual temperature
t	time
u	radial velocity of air
V_r	representative terminal velocity of rain relative to the air
w	vertical velocity of air
Z_H	height of integration domain
z	vertical coordinate
Γ_d	dry adiabatic lapse rate
η	vorticity
ν	coefficient of eddy diffusion
$\bar{\rho}$	air density of environmental basic state
ψ	streamfunction
Δr	radial grid interval
ΔT_h	temperature excess at the center of a heat island
Δt	time increment
Δz	vertical grid interval
Barred variables represent an environmental basic state.	

1. INTRODUCTION

1-1 *Background and Purpose of the Study*

Meteorological and climatological conditions are different in urban areas from those in their surroundings, and this is recognized as a result of the fact that man inadvertently modifies the conditions of the environment through urbanization. Since motions in the boundary air layer are closely controlled by the nature of the earth's surface, urbanization can more or less cause meteorological and climatological changes in the boundary air layer. The most remarkable anomaly caused by urban influence is that a city has a higher temperature than its surroundings. This phenomenon is called an urban heat island.

A great deal of attention has been devoted to the urban effects on precipitation. These effects have been noted for a number of decades but were relatively hard to verify. The reason for this is the very high variability of rain amount and the poor quality of the ordinary raingauge network as a sampling device. These problems have yet to be resolved (Chandler, 1970 ; Sekiguti, 1970 ; Daigo and Nagao, 1972 ; Yoshino, 1975).

Precipitation anomalies caused by urban influences were postulated first by Schmauss (1927) and by Ashworth (1929). Since then, urban effects on precipitation have been noted for a number of decades. Many studies have shown that cities can aggravate severe weather activity and measurably alter precipitation in and downwind of them (Changnon, 1968 ; Hobbs et al., 1970a ; Atkinson, 1971 ; Huff and Changnon, 1972 ; Khemani and Murty, 1973 ; Sanderson et al., 1973 ; Schickedanz, 1974 ; Dettwiller and Changnon, 1976 ; Changnon, 1978 ; Sanderson and Gorski, 1978). However, there have

been some investigations that have questioned the nature and the magnitude of the urban effects on precipitation (Spar and Ronberg, 1968; Ogden, 1969; Holzman and Thom, 1970; Harman and Elton, 1971; Holzman, 1971a; 1971b; Pittcock, 1977; Lowry and Probal, 1978).

If precipitation and aggravation of severe weather activity really increase in urban areas, two meanings can be obtained: 1) It demonstrates the possibility of rain making and 2) it presents a serious problem with regards to flood prevention. Studies on weather modification, such as rain making, have been carried out for more than 40 years, but have yet to be arrived at sound conclusions. Therefore, it would make a valuable contribution to the development of weather modification if the urban effects on precipitation were clarified.

When structures are designed for the prevention of rainfall disasters, a design rainfall is used as an inalterable factor. The design rainfall for a certain return period is determined by a probability analysis. For example, rivers in urban areas are commonly designed not to flood due to heavy rainfall, once in thirty years or less. This has significance only when a heavy rainfall occurs with a certain frequency which can be estimated from a series of observed data obtained over a long period of time. Therefore, if cities aggravate severe weather activity, and urbanization affects the change of the frequency of occurrence of heavy rainfall, it will be necessary to establish another fundamental principle in flood disaster prevention.

Three factors are considered to be capable of inducing precipitation anomalies in an urban area. These are: (i) atmospheric destabilization from the output of the urban heat island, (ii) modification of cloud physical processes through the addition of condensation and ice nuclei from a city, and (iii) mechanical production of confluence zones over a city.

As mentioned above, urban effects on precipitation have not yet been clarified, and it is both scientifically and practically needed to clarify these urban effects. The purpose of the present study is to show that an urban heat island can aggravate convective storms.

Urban effects on the occurrence of heavy rainfall will be studied from three different approaches. First, a theoretical study will show that a heat island modifies the atmosphere to be favorable for the development of a convective cloud which produces heavy rainfall when it develops well. Next, some case studies obtained from the Tokyo metropolitan area, when the highest and second highest values of 60 minutes rainfall were recorded, will be presented and analyzed. This analysis will show that the heat island actually has an effect on the occurrence of heavy precipitation. Last, statistical studies will show that the heat island effect on precipitation is large and that the heat island can be a predominant causative factor in the occurrence of convective precipitation.

1-2 *Review of Previous Studies*

The fact that there are changes in the atmospheric environment of cities was recognized many years ago. As early as 1818, Luke Howard clearly established that the city of London had a higher temperature than the nearby countryside (Yoshino, 1975; Landsberg, 1981). He offered an explanation by citing the large amount of heat given off

by coal-fired domestic heating and manufacturing processes. Toward the beginning of this century, changes of other meteorological elements in urban areas such as wind and rainfall were reported. A history of studies on city climates was given in detail in the classical work by Kratzer (1937).

In the 1930's, detailed observation became possible with the introduction of motor vehicles as instrument carriers for traveling across cities to ascertain a variation of meteorological elements in metropolitan areas. Since then, observations of temperature have been made in many cities in Europe, the U. S. A., Japan and other countries (Sundborg, 1950; Duckworth and Sandberg, 1954; Sekiguti, 1960; Kawamura, 1964; Chandler, 1965; Bornstein, 1968; Sharon and Koplowitz, 1972). These observations have established that a city's temperature pattern often stands out boldly in relation to a fairly uniform rural temperature field. A city is always warmer than its surroundings, a phenomenon that has been given the graphically descriptive label "urban heat island".

As for urban precipitation anomalies, only a few studies have been made. As has been mentioned, Schmauss (1927) and Ashworth (1929) called attention to the urban precipitation anomalies caused by urban influence. They noted an 11% increase of mean annual precipitation for the eastern part of Munich, Germany. In addition, Asworth's research showed the weekly variation of precipitation in an industrial town.

A few studies on the urban precipitation anomalies were made in cities in Japan. Fukui and Koizumi (1938) drew a conclusion of no anomalies being present from special observation in the Tokyo area from July to November except in August. The total amount of drizzle, however, was shown to be greater by 50-100 mm in the Tokyo urban area (Yoshino, 1957), and the number of drizzle days increased in accordance with the development of cities in many cities in Japan and other countries (Yoshino, 1977).

In 1968, an urban anomaly at La Porte, U. S. A., was reported (Changnon, 1968). It was found that La Porte had 31% more precipitation, 38% more thunderstorms, and 246% more hail days than the surrounding stations. This report created considerable scientific and public concern as to whether there could be measurably altered precipitation and severe weather in and down-wind of cities, and a controversy resulted over the reality of the La Porte anomaly (Ogden, 1969; 1971; Changnon, 1970; 1971; Holzman and Thom, 1970; Hidore, 1971; Holzman, 1971a; 1971b; Charton and Harman, 1973; Fritts and Ashby, 1973).

The interest created led to climatological studies of other cities. Historical weather records at eight U. S. cities were studied for indications of inadvertent precipitation modification. It was shown that the six largest cities, such as Washington D. C., Houston, New Orleans, Chicago, Cleveland and St. Louis, had precipitation increases of 10-30% in and downwind of their urban areas, associated increases in thunderstorm and hailstorm activities (Huff and Changnon, 1973). Subsequent studies in the Detroit area showed that urban effects on precipitation were seen in the summer (Sanderson et al., 1973; Sanderson and Gorski, 1978). A study of the urban industrial complex in Bombay, India, showed that the region downwind of the urban industrial complex received about 15% more rainfall from 1941 to 1969, which is the period of increased industrialization (Khemani and Murty, 1973). Urban effects on local convective precipitation were suggested in Paris, St. Louis and Chicago (Dettwiller and Changnon, 1976).

Weekly variation of precipitation was found to be another urban anomaly of

precipitation. In an industrial town, Rochdale, England, weekdays had 20% more precipitation than Sundays on the average, compared to the nearby stations where this difference was small (Ashworth, 1929). The weekly precipitation for Paris showed a gradual increase from Monday to Friday with a sharp drop on weekends. The difference was significant at the 95% confidence level (Dettwiller, 1970). A similar weekly cycle was also reported to be fairly significant for London (Lawrence, 1971). These findings suggested that human activities produce some effects on precipitation in an urban area.

Contradictory results, however, were also obtained. At non-urban Brighton, greater rainfall was recorded on weekdays (Nicholson, 1969), but greater rainfall was recorded on weekends at Norwich (Norgate, 1974) and Irchester (Carrea, 1975). An alternative explanation for the weekly variation of precipitation is that it can be evidence of a natural tendency for quasi-periodicities of about a week, a hypothesis suggested by Namias (1966).

The project METROMEX (METROpolitan Meteorological EXperiment), which aimed at studying the reality and causes of urban anomalies of precipitation in St. Louis, revealed the following anomalies. An urban-induced increase in the average summer rainfall ranged from 6–15%, and the urban-induced mechanism was apparently most active on days of moderate to heavy intensities in the natural rainfall (Huff and Changnon, 1972). For cells occurring in the urban-industrial zone, the average rainfall volume was 176% greater than for cells in the control sample (Schickedanz, 1974). Severe local storm activities also increased in and downwind of the city (Changnon, 1978). Radar studies indicated the maximum enhancement in the first echo formation (Braham and Dungey, 1978) and a substantial enhancement in the frequency of tall echoes over the city and near downwind areas (Braham and Wilson, 1978). Urban echoes were also found to be thicker than their rural counterparts (Ochs and Johnson, 1980).

A few investigations sought causes of these rainfall anomalies through case studies. In these, an individual rain event is examined for antecedent meteorological conditions that can be related to an urban effect on the rainfall, tracing links between the presence of an urban area and the anomalous precipitation event. Parry (1956) cited an occurrence in Reading, England. It is a prototype for such an induction of rainfall, which yielded 34.5 mm in two hours over the city and only 2.5mm in the rural area. Atkinson (1971) undertook a detailed case study of a thunderstorm which rapidly grew over the London city and produced local heavy rainfall there. Parry (1956) related the anomalous rain amounts over the city to a heat island existed prior to the rainshower, and Atkinson (1971) also explained that the cloud growth was due to the warmer air over the city. Harnack and Landsberg (1975) showed that urban thermal factors caused anomalous rainfall distribution of isolated summer showers in the Washington, D. C. area. The direct effect of the surface temperature patterns on the initiating of a cumulus was indicated also by means of numerical simulation (Ochs, 1975).

Atmospheric pollution is considered to cause urban anomalies, since some pollutants work as cloud condensation nuclei. Hobbs et al. (1970a) and Changnon (1971) pointed out that air pollution causes an increase in rainfall. On the other hand, Ogden (1969) and Lowery and Probal (1978) reported that such effects were not noticed in industrial areas, and that a reduction of rainfall was shown over areas where sugar-cane burning was practiced (Warner, 1968). Elliott and Ramsey (1970) questioned Hobbs' results, against

which there was an argument by Hobbs et al. (1970b). Studies by means of numerical experiments indicated that concentration of cloud condensation nuclei did not cause either an increase in rainfall (Hindman et al., 1977) nor development of clouds (Ochs and Semonin, 1979).

As described above, day-of-the-week analyses for various urban and rural areas were contradictory, and climatological analyses of the effects of the concentration of cloud condensation nuclei showed diversity. Spar and Ronberg (1968) have noted a decrease in precipitation at the Central Park Station in the middle of Manhattan, New York. Harman and Elton (1971) have suggested an alternative explanation for the La Porte anomaly in terms of the location of a lake breeze convergence zone in the vicinity of La Porte and its movement under the influence of changing mean winds. Pittcock (1977) has suggested that natural changes in the general circulation, locally enhanced by topography, largely account for changes which had been ascribed to pollution in the Washington State area.

There are many meteorologists and climatologists who have questioned the nature and magnitude of anthropogenic effects on phenomena with precipitation. More detailed analytical, statistical and quantitative treatments are needed for those effects to be accurately and confidently assessed, and such studies have been urged (Chandler, 1970 ; Sekiguti, 1970 ; Daigo and Nagao, 1972 ; Yoshino, 1977).

2. THEORETICAL STUDY

This chapter concerns the effects of a heat island on the development of a convective cloud which causes heavy precipitation when it develops well from a theoretical point of view. The atmosphere is assumed to be conditionally unstable, as is usually observed.

Since a convective cloud develops better as the atmosphere is more unstable in degree and the energy source of convective activity is the latent heat released by condensation of water vapor transported from the subcloud layer, the heat island is logically considered to enhance the development of a cloud in two ways : the destabilization of static stability of the atmosphere and an induction of an upward motion over the heat island.

The heat island induces a local circulation which consists of the low level inflow to the island, the rising current above it and the upper return flow. This circulation is observed in the boundary layer, and a convective cloud forms above the boundary layer. Therefore, the purpose of this chapter is to study the effects of the conditions in the subcloud layer on the development of the cloud. Little has been studied concerning these effects, though relation between the size and spacing of clouds and random surface heating have been studied (Hill, 1974). Numerical experiments and an analysis from the energy budget viewpoint is conducted, as described in the following section.

2-1 *Numerical Experiment*

First, the development of the convective cloud over the heat island is studied by means of numerical simulation.

2-1-1 Numerical model

(1) Assumptions

The following assumptions are made.

- (i) The effect of general wind is not included. The vertical shear in the general wind has been theoretically shown to inhibit cumulus convection (Kuo, 1963; Asai, 1964).
- (ii) The heat island is initially given, and no account is taken of the physical processes causing it.
- (iii) No account is taken of the vertical structure of the atmosphere. It will be shown, however, that the heated area at the surface generates a vertical temperature field which possesses characteristics of those observed in urban areas, as known from numerical studies already conducted on heat islands (e.g. Delage and Taylor, 1970).
- (iv) The heat island is circular.
- (v) Temperature at the surface in the heat island is kept constant with time unless evaporation occurs there.
- (vi) All eddy diffusion coefficients are the same and constant in both time and space ($50\text{m}^2/\text{s}$ in almost all cases).
- (vii) Motions are anelastic (Ogura and Phillips, 1962).
- (viii) The cloud physical processes are parameterized following Kessler (1969).
- (ix) All supersaturated water vapour condenses, and cloud water in the unsaturated region evaporates instantaneously until saturation is realized in the region.
- (x) Rainwater in the unsaturated region evaporates proportional to the saturation deficit at a constant rate of $10^{-3}/\text{s}$ following Yoshizaki (1978).

(2) Equations

Assumptions (i) and (iv) signify that motion is axisymmetrical, and so a cylindrical coordinate is used. The vorticity equation, conservation of total water substance, the first law of thermodynamics, a water vapour equation, and a cloud water equation are given as:

$$\frac{\partial \eta}{\partial t} = -u \frac{\partial \eta}{\partial r} - w \frac{\partial \eta}{\partial z} + \left(\frac{2w}{\bar{\rho}} \frac{\partial \bar{\rho}}{\partial z} + \frac{u}{r} \right) \left(\eta - u \frac{\partial \bar{\rho}}{\partial z} \right) + uw \frac{\partial^2 \bar{\rho}}{\partial z^2} - \bar{\rho} g \frac{\partial}{\partial r} \left(\frac{T_v}{T_v} - Q_t \right) + \frac{\bar{\rho} g}{\bar{P}} \frac{\partial (P - \bar{P})}{\partial r} + \nu \left(\frac{1}{r} \frac{\partial}{\partial r} r \frac{\partial \eta}{\partial r} + \frac{1}{\bar{\rho}} \frac{\partial}{\partial z} \bar{\rho} \frac{\partial \eta}{\partial z} - \frac{\eta}{r^2} \right), \quad (2-1)$$

$$\frac{\partial Q_t}{\partial t} = -u \frac{\partial Q_t}{\partial r} - w \frac{\partial Q_t}{\partial z} + \frac{1}{\bar{\rho}} \frac{\partial}{\partial z} (\bar{\rho} V_r Q_r) + D_{q_v + q_c}, \quad (2-2)$$

$$\frac{\partial T}{\partial t} = -u \frac{\partial T}{\partial r} - w \left(\frac{\partial T}{\partial z} + \Gamma_d \right) - \frac{L_e}{c_p} P_e + D_\tau, \quad (2-3)$$

$$= \left\{ -u \frac{\partial T}{\partial r} - w \left(\frac{\partial T}{\partial z} + \Gamma_d \right) + \frac{L_e}{c_p} \frac{\partial q_a}{\partial t} + D_\tau \right\} / \left(1 + \frac{L_e^2 q_s}{c_p R_v T^2} \right)$$

in a saturated region, (2-4)

$$\frac{\partial Q_v}{\partial t} = -u \frac{\partial Q_v}{\partial r} - w \frac{\partial Q_v}{\partial z} + P_e + D_{q_v} \quad \text{in an unsaturated region,} \quad (2-5)$$

$$= \frac{\partial q_s}{\partial t} \quad \text{in a saturated region,} \quad (2-6)$$

$$\frac{\partial Q_c}{\partial t} = -u \frac{\partial Q_c}{\partial r} - w \frac{\partial Q_c}{\partial z} + P_c - P_r + D_{qc}, \quad (2-7)$$

where a diffusion term of variable f is

$$D_f = \nu \left(\frac{1}{r} \frac{\partial}{\partial r} r \frac{\partial f}{\partial r} + \frac{1}{\bar{\rho}} \frac{\partial}{\partial z} \bar{\rho} \frac{\partial f}{\partial z} \right). \quad (2-8)$$

The derivation of these equations is explained in Appendix A.

Cloud physical processes are represented by P_e (evaporation rate of cloud water or rainwater), P_c (condensation rate or evaporation rate of cloud water) and P_r (rate of change of cloud water to rainwater). Rainwater, Q_r , is produced through two processes, autoconversion and collection, which are represented by Kessler's formula (2-9) with the parameters $k_1=0$ for $Q_c < 10^{-3}$, and $k_1=10^{-3}$ for $Q_c > 10^{-3}$, after Soong and Ogura (1973).

$$P_r = k_1 (Q_c - 10^{-3}) + 2.2 \cdot Q_c \cdot Q_r^{0.875} \quad (2-9)$$

where

$$Q_r = Q_t - Q_v - Q_c. \quad (2-10)$$

The horizontal velocity, u , and vertical velocity, w , can be determined by solving Eqs. (2-11) and (2-12) with boundary conditions shown in the next section.

$$\eta = \frac{\partial \bar{\rho} u}{\partial z} - \frac{\partial \bar{\rho} w}{\partial r} = \frac{1}{r} \frac{\partial^2 \psi}{\partial z^2} + \frac{\partial}{\partial r} \left(\frac{1}{r} \frac{\partial \psi}{\partial r} \right), \quad (2-11)$$

$$r \bar{\rho} u = \frac{\partial \psi}{\partial z}, \quad r \bar{\rho} w = - \frac{\partial \psi}{\partial r}. \quad (2-12)$$

The term $(\bar{\rho} g / \bar{P}) \partial P / \partial r$ in Eq. (2-1) is obtained by Eq. (2-13) using the backward time scheme and assuming $\partial P / \partial r = 0$ initially.

$$\frac{\partial u}{\partial t} = -u \frac{\partial u}{\partial r} - w \frac{\partial u}{\partial z} - \frac{1}{\bar{\rho}} \frac{\partial P}{\partial r} + \nu \left(\frac{1}{r} \frac{\partial}{\partial r} r \frac{\partial u}{\partial r} + \frac{1}{\bar{\rho}} \frac{\partial}{\partial z} \bar{\rho} \frac{\partial u}{\partial z} - \frac{u}{r^2} \right). \quad (2-13)$$

(3) Boundary conditions

The top, bottom and lateral boundaries are assumed to be rigid and slip:

$$\frac{\partial \bar{\rho} u}{\partial z} = 0, \quad w = 0. \quad (2-14)$$

$$u = 0, \quad \frac{\partial w}{\partial r} = 0. \quad (2-15)$$

Since the motion is axisymmetrical, Eqs. (2-16) and (2-17) are obtained at $r=0$:

$$u = 0, \quad \psi = 0, \quad \eta = 0, \quad (2-16)$$

$$\frac{\partial T}{\partial r} = \frac{\partial w}{\partial r} = \frac{\partial Q_t}{\partial r} = \frac{\partial Q_v}{\partial r} = \frac{\partial Q_c}{\partial r} = 0. \quad (2-17)$$

Equation (2-16) is adopted as the boundary condition at $r=0$ for u , ψ , η . For other variables no boundary condition at $r=0$ is given. In computing the term of $(1/r)(\partial f / \partial r)$, however, relation (2-18), which is satisfied when $\partial f / \partial r|_{r=0} = 0$, is used.

$$\frac{1}{r} \frac{\partial f}{\partial r} \Big|_{r=0} = \frac{\partial^2 f}{\partial r^2}. \quad (2-18)$$

It is apparent from Eqs. (2-15) and (2-16) that $\psi=0$ and $\eta=0$ at all boundaries.

Surface temperature is assumed constant with time, unless liquid water evaporates at the surface. For the temperature at $z=Z_H$ and $r=R_L$ and the content of the total water substance, water vapour content and cloud water content at $z=0$, Z_H and $r=R_L$,

no boundary assumption is made. In computing diffusion terms, however, the horizontal derivatives of these variables at the lateral boundary and vertical derivatives at the top and bottom boundaries are put to zero to avoid fictitious diffusion across the boundaries.

(4) Schemes

Calculations are performed with 81 by 56 rectangular grids having a width of 20 km ($\Delta r = 250\text{m}$) and a depth of 11km ($\Delta z = 200\text{m}$). In an exceptional case, the depth is 5.5km and $\Delta z = 100\text{m}$. The forward time scheme adopted, except for computing $\partial P / \partial r$, and the time increment is 10 sec in most cases. Advective terms are handled by the upstream difference, and the centered difference is used for space derivatives other than advection terms.

2-1-2 Initial conditions

Numerical simulations are made for 14 cases. The development of a cloud without a heat island is computed for Case 1. The developments of a cloud over a layer modified by a heat island with a different radius are computed for Cases 2-6. The life of a cloud from initiation by the heat island is simulated in Cases 7-14.

In Cases 1-6, the initial disturbance of a cloud is given in the domain $0 \leq r \leq 2\text{km}$ and $1 \leq z \leq 2\text{km}$. The initial disturbance is that the relative humidity is 100% and the temperature excess is $\Delta T_c(r, z) = 0.3(1 - r^2/2^2)(1 - (z - 1.5)^2/0.5^2)^\circ\text{C}$. The heat islands in Cases 2-6 are given as of a radius $r_h\text{km}$ and of a surface temperature excess $\Delta T_h(r) = \Delta T_h(1 - r^2/r_h^2)^\circ\text{C}$ at $r \leq r_h$. Two values of r_h and ΔT_h in each case are listed in Table 2-1 with other conditions.

In Cases 2-6, the initial disturbance is given when the circulation induced by the heat island is in its most developed stage. Namely, the initial states in Cases 2-6 are those calculated as follows: the heat island generates circulation in the same environmental basic state as that in Cases 7-14 described below. The developments of the circulations are simulated, and the states when the maximum vertical velocity shows a peak are adopted as the initial states. For example, the maximum vertical velocities of the circulation induced by the heat island with $r_h = 3\text{km}$ and $\Delta T_h = 1.2^\circ\text{C}$ are 0.80m/s from 41 through 43 min, 0.81m/s from 44 through 46 min and 0.80m/s from 47 through 50 min. The states at 45 min are chosen as the initial states in Case 3.

Air is at rest at the initial time in Cases 1 and 7-14. Vertical profiles of temperature and relative humidity are the same in these cases. They are determined with reference to aerological data in the summer at the Tateno Aerological Observatory, Japan, and are shown schematically in Fig. 2-1. The temperature is 20°C at $z = 1\text{km}$ where the pressure is 900mb. Temperature lapse rate is 7°C/km at $z \leq 1\text{km}$, and 6°C/km above $z = 1\text{km}$. The mixing ratio is the same horizontally, so that relative humidity decreases with the approach of the center of the heat island. Relative humidity in the environmental basic atmosphere is 80% at $z \leq 1.4\text{km}$, and it decreases at the rate of $7.5\%/ \text{km}$ above $z = 1.4\text{km}$. For Case 1, the surface temperature is 28.2°C , which is equal to that at the center of the heat island in Cases 2-6.

The horizontal scale of the heat is different between Cases 7-11 (see Table 2-1). The horizontal distribution of the surface temperature in the heat island in Case 12 is $\Delta T_h(r) = \Delta T_h$ at $r \leq r_h$ which is different from that in other cases. As known from the formula, the heat island induces circulation which concentrates over its center in cases with a type

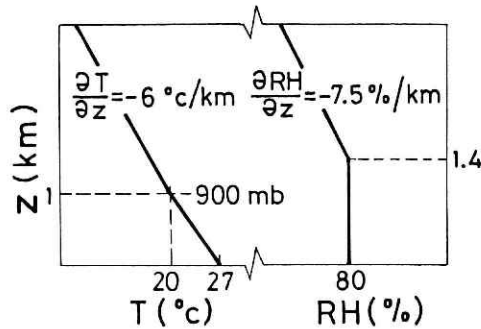


Fig. 2-1 Vertical profiles of temperature (left) and relative humidity (right) in the basic state.

Table 2-1 Initial conditions.

case	disturbance of cumulus	heat island			air motion
		r_h (km)	ΔT_h (C)	type	
1	given			none	at rest
2	"	1	1.2	I	circulated
3	"	3	"	"	"
4	"	6	"	"	"
5	"	12	"	"	"
6	"	18	"	"	"
7	not given	1	2.0	"	at rest
8	"	3	"	"	"
9	"	6	"	"	"
10	"	12	"	"	"
11	"	18	"	"	"
12	"	3	"	II	"
13	same as Case 8 except diffusion term				
14	same as Case 8 except $\Delta z=100$ m				

The type symbols are: I, $\Delta T_h(r) = \Delta T_h(1 - r^2/r_h^2)$ $r \leq r_h$;

II, $\Delta T_h(r) = \Delta T_h$ $r \leq r_h$.

I heat island, while this does not hold true for Case 12. The initial conditions of Cases 13 and 14 are the same as Case 8, but the model is different. No diffusion is assumed after 5 min in Case 13. In Case 14, $\Delta z = 100$ m and $Z_H = 5.5$ km are used.

2-1-3 Results

(1) Comparisons of the results for Cases 1-6

Development of the initial disturbance of a cloud and some features of the air motion field and the cloud are compared between Cases 1-6. The comparisons show that the heat island modifies the atmosphere to an extent that a cloud can noticeably develop over it, though magnitudes of the heat island's effects are different from each other.

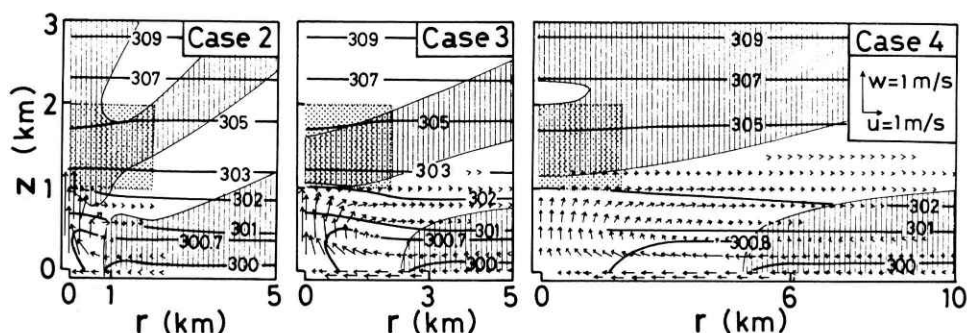


Fig. 2-2 Initial states in Cases 2-4. Potential temperatures are shown in unit of K by contours, and air motion is shown by wind vectors and hatching. A wind vector is not drawn where both $|u|$ and $|w|$ are less than 0.1 m/s, and hatching indicates an area with downward motion. Dots indicate a cumulus disturbance.

As described in the previous section, the initial states in Cases 2-6 are those at a time when the circulations induced by the heat islands are at their most developed stage. The potential temperature at the center of the heat island is 300.9°K and is equal to that at about $z=0.4$ km. Initial fields of air motion and potential temperature are characterized by the following (i)–(iii) in Cases 2-4 (see Fig. 2-2). (i) The top of the main circulation is about 1 km, which corresponds to the height of the base of the initial disturbance. (ii) Downward motion occupies a large part of the domain where the initial disturbance is given, though the value is small. (iii) Potential temperatures are lower at levels between 0.5 and 1.0 km over the heat island than in its surroundings. The phenomenon (iii) is observed over urban heat islands and is known as “cross-over” (e.g., Garstang, et al., 1975).

Figure 2-2 also shows that there are differences in the air motion field in three cases. In Case 2 where $r_h=1$ km, the area of updraft is the smallest and the maximum vertical velocity (1.5 m/s at $r=0$ and $z=0.4$ km) is the largest among the three. In Case 3 where $r_h=3$ km, an updraft is formed in the whole area under the base of the disturbance. The maximum vertical velocity is 0.8 m/s at $r=0$ and $z=0.4$ km. In Case 4 where $r_h=6$ km, a weak updraft is formed in a wide area with a radius of 5 km. The maximum updraft is 0.3 m/s at the same position as in Cases 2 and 3. The area with a high potential temperature in the lower layer is the largest in Case 3.

Initial states in Cases 5 and 6 show different features from those in Cases 2-4. The cross-over is not obvious in Cases 5 and 6. The temperature is slightly higher over the heat island. As for the air motion field, vertical velocity is very small and the area over which the updraft is formed is as wide as more than 10 km in radius. The maximum vertical velocity is 0.14 m/s in Case 5 and it is less than 0.1 m/s in Case 6. These findings suggest that upward motion induced by the heat island is so weak that the temperature field is not remarkably modified.

Figure 2-3 shows the air motion field, cloud shape and area with rainwater at 15 min in Cases 1-6. There are noticeable differences in the spatial features among four of the cases. It demonstrates that the development of the initial disturbance is promoted by the

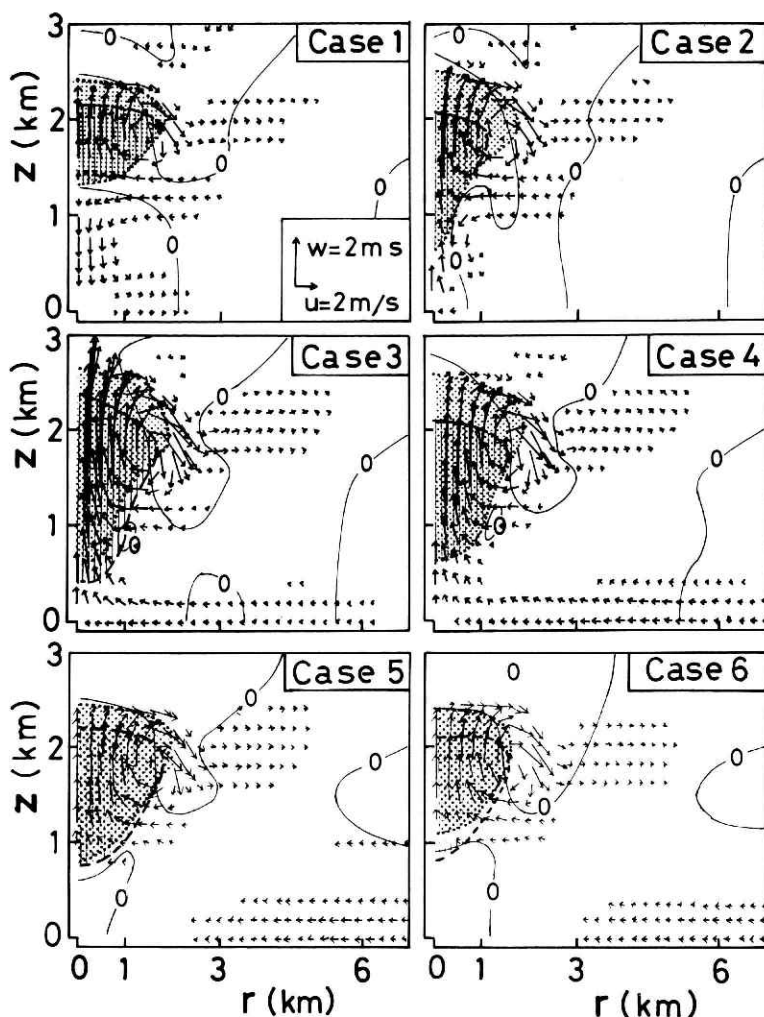


Fig. 2-3 Vertical cross-sections of air motion, a cloud and an area with rainwater at 15 min in Cases 1-6. A wind vector is not drawn where both $|u|$ and $|w|$ are less than 0.3m/s, and at $r=0$ in the cloud in Cases 2-4. The boundaries between upward motion and downward motion, i.e., contours of $w=0$, are shown by thin lines. Dots and hatching indicate a cloud and an area with rainwater, respectively.

heat island.

In Case 1 where no heat island is given, a downward motion is formed under the cloud base, and it produces a divergent field near the surface. As is well known, the weight of accumulated liquid water causes downdraft when a cumulus develops (e.g., Byers and Braham, 1949; Srivastava, 1967). In Case 1, however, the weight of liquid water has little effect on the formation of the downward motion, since no liquid water exists at levels under the cloud base. The air motion field shows that the atmosphere is so stable that the initial disturbance cannot form a steady upward motion in the subcloud layer, though surface temperature is equal to that at the center of the heat island in Cases

Table 2-2 Results of Cases 1-6.

Case	W_{\max} (m/s)	P_1 (mm)	P_2 (mm)
1	3.3	--	--
2	10.5	9.6	1.9
3	17.0	28.2	8.2
4	14.8	21.0	5.8
5	9.2	5.0	0.9
6	7.9	2.5	0.2

Symbols are: W_{\max} , maximum vertical velocity in a space-time field; P_1 and P_2 , total amounts of rain at $r=0$ and $r=0.75$ km, respectively.

2-6.

In Case 2, a strong updraft forms in a narrow area of $r \leq 0.25$ km and a downward motion forms in $0.75 \leq r \leq 2.75$ km at lower levels. The maximum vertical velocity is 1.1 m/s in Case 1, 4.4 m/s in Case 2, 5.4 m/s in Case 3 and 2.5 m/s in Case 4. The largest vertical velocity is recorded in Case 3. In Case 3, the area with strong updraft is not so small as in Case 2 and downward motion is not initiated in the subcloud layer even though rainwater falling out of the cloud reaches a height of 0.4 km over the center. In Case 4, vertical velocities around $r=0$ are not so large as those in Case 2, while the area where vertical velocity exceeds 2 m/s is wider than in Case 2.

The initial disturbance of the cumulus expands downward around $r=0$ in Cases 2-4. The width of the expansion is the smallest in Case 2 and the largest in Case 4. Comparisons of air motion and the cloud shape between Cases 1-4 show that air motion in the lower layer is controlled mainly by the heat island and the upward motion induced by the heat island is introduced to the motion induced by the cloud.

Air motion fields in Cases 5 and 6 have different features from those in Cases 2-4. Downward motions and divergent fields are formed under the cloud bases like in Case 1, though magnitudes are not as large as those in Case 1. Upward motions induced by the heat islands are not as strong as those in Cases 2-4.

The initial disturbance dissipates without developing well in Case 1. While, the disturbances develop well and produce rain in Cases 2-6, though the degrees of development are different in each case (see Table 2-2). Up to a 3 km radius of the heat island, it is shown that the heat island enhances convective activity more as the heat island becomes larger. The maximum vertical velocity in the space-time field and the total amount of rain at $r=0$ and $z=0$ are 3.3 m/s and no rain in Case 1, 10.5 m/s and 9.6 mm in Case 2, 17.0 m/s and 28.2 mm in Case 3. When the radius of the heat island is larger than 6 km, cumulus convection becomes less active as the heat island becomes larger. The maximum vertical velocity and total amount of rain are 14.8 m/s and 21.0 mm in Case 4, 9.2 m/s and 5.0 mm in Case 5, and 7.9 m/s and 2.5 mm in Case 6.

(2) Comparisons of results for Cases 7-11 and 13

The heat island initiates the cloud over it in Cases 7-14. The surface temperature is higher by 2°C at the center than in the surroundings. The potential temperature at the center is 301.6°K and this is equal to that at a height of about 0.8 km. The results show that clouds which form over heat islands with different horizontal scales behave differently.

Figure 2-4 shows time-height variations of vertical velocity, potential temperature and a cloud boundary at $r=0$ in Cases 7-9 and 13. A comparison is made first between

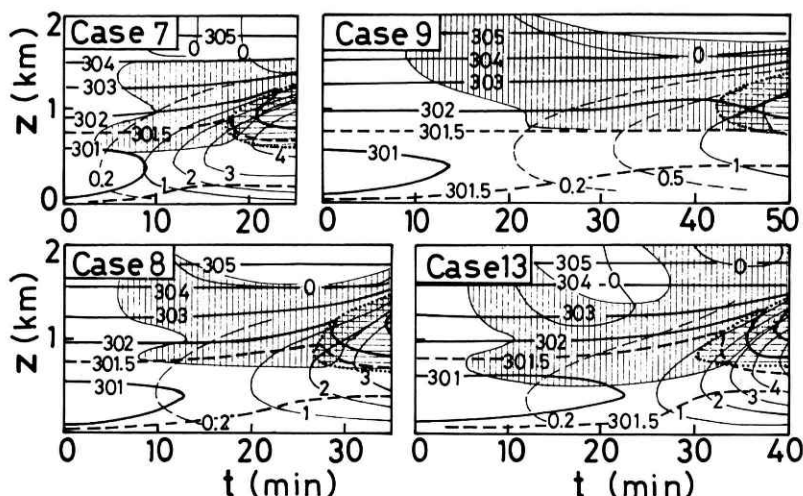


Fig. 2-4 Time-height cross-sections of vertical velocity, potential temperature and a cloud boundary in Cases 7-9 and 13. Thin lines show vertical velocity (m/s) and thick lines potential temperature ($^{\circ}K$). Vertical hatching indicates an area where potential temperature is lower than the initial value, and horizontal hatching a cloud. Thick broken lines are contours of $301.5^{\circ}K$.

Cases 8 and 13. There is no difference in initial conditions and the numerical models except in the diffusion term: no diffusion is assumed after 5 min in Case 13. If no diffusion was assumed from the beginning, the heat island initially given could not disturb the atmosphere.

The heat island initiates the cloud around $z=0.8\text{km}$ over the center at 27 min in Case 8 and at 30 min in Case 13. There are differences between Cases 8 and 13: the time when a cloud forms is later in Case 13 by 3 min; the maximum vertical velocity exceeds 1m/s at an earlier time in Case 8 and others. But these differences are not essential for the purpose of this study and they are also slight when a comparison is made between the differences arising between Cases 8 and 13 and those between Cases 7-11, as described below. This shows that the motion induced by a heat island contributes most to the modification of the lower layer and the initiation of the cloud, and the contribution of diffusion is negligibly small.

Heat islands with different radii modify the lower layer and initiate the cloud in the same manner. The heat island generates upward motion over it. The air motion develops a virtually isothermal layer below about $z=0.8\text{km}$. Penetration of accelerated dry air into the conditionally unstable layer causes a temperature lower than the initial value above about $z=0.8\text{km}$. The upward motion induced by the heat island can transport water vapour enough to initiate the cloud and to produce a positive buoyant force in it.

Because the surface temperature at the center is the same in Cases 7-11, $\partial T/\partial r$ becomes larger as the radius of the heat island is smaller. Therefore, $\partial\eta/\partial t$ becomes larger, and a larger velocity is induced at an earlier time as the radius of the heat island is smaller. Thus, vertical velocity and potential temperature varies more rapidly with

time and the cloud is initiated at an earlier time in Case 7 than in Case 8, and in Case 8 than in Case 9, and so on. Besides this, there is not any essential difference in the way of the initiation of the cloud among Cases 7-11, so the time-height cross-sections in Cases 10 and 11 are not shown in the figure.

There are differences in spatial features and cloud development among Cases 7-11. A heat island with a small horizontal scale initiates a cumulus with a small horizontal scale (see Fig. 2-5). At 15 min after a cloud initiation, vertical velocity and temperature in the cloud are the largest in Case 8 among Cases 7-11. They are the smallest in Case 11 where the heat island is the largest. Upward motion with a low value is generated over a wider area and the surface temperature at the center is the highest in Case 11. Advection most notably decreases the temperature at lower levels over the center in Case 7 where the horizontal scale of the heat island is the smallest.

Figures of some variables indicating characteristics of the initiation of the cloud and its development in Cases 7-11 are summarized in Table 2-3. The cloud develops the best and the amount of rain recorded at the center is the largest in Case 9, where the radius of the heat island is neither the largest nor the smallest. In Case 11, where the heat island is 18km in radius, a cloud is formed but does not develop well. The results show that the heat island can initiate a cloud which develops well to produce much rain at the surface when the heat island is neither very large nor very small.

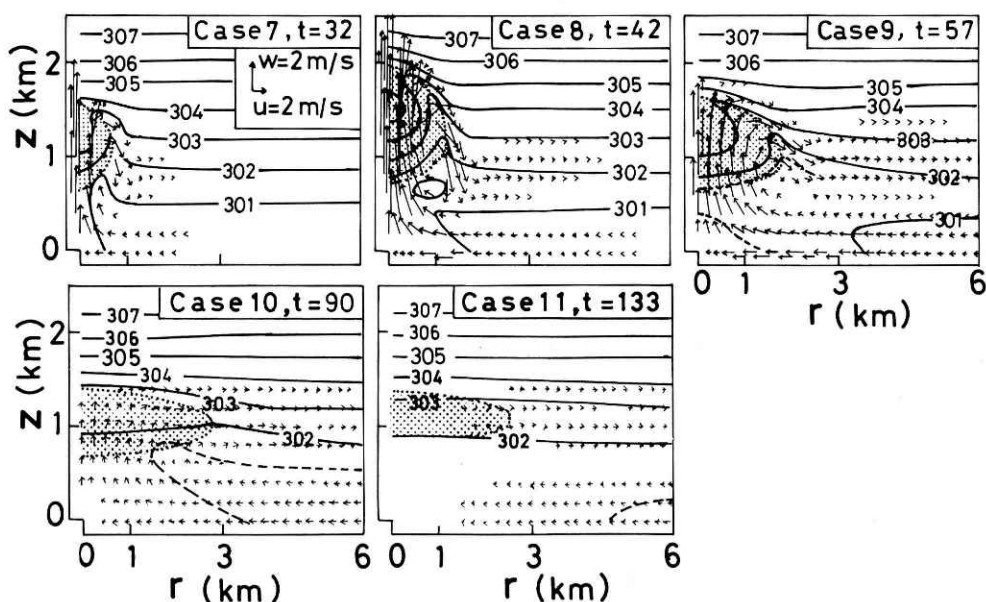


Fig. 2-5 Vertical cross-sections of air motion, potential temperature and a cloud at 15 min after cloud initiation in Cases 7-11. A wind vector is not drawn where both $|u|$ and $|w|$ are less than 0.3 m/s. Contours of potential temperature in the cloud and near the cloud base in Case 8 indicate 305 °K and 301 °K, respectively. Broken lines in Cases 9-11 indicate 301.5 °K. The dotted area shows a cloud.

Table 2-3 Results of Cases 7-11.

Case	t_i (min)	W_{max} (m/s)	P_1 (mm)	P_2 (mm)
7	17	7.1	2.6	--
8	27	15.3	11.7	0.0
9	42	17.9	21.5	0.7
10	75	14.8	11.4	3.3
11	118	0.3	--	--

Symbols are: t_i , time when a cumulus forms;
 W_{max} , maximum vertical velocity in a space-time
field; P_1 and P_2 , total amounts of rain at $r=0$
and $r=7.5$ km, respectively.

(3) Results of Case 12

In the case of $\partial T/\partial r=0$ in the heat island, air concentrates near the boundary of the heat island because $\partial T/\partial r$ is largest there. The zone where air concentrates moves gradually toward the center of the heat island in the same manner as studied by Delage and Taylor (1970). The motion of the circulation affects the location where the cloud is initially formed and its development.

In Case 12, the maximum vertical velocity is larger at an early stage than in Case 8. The maximum vertical velocity is 1.59m/s, and its location is at $r=2.5$ km and $z=0.4$ km at 20 min in Case 12, while it is 0.96m/s at $r=0$ and $z=0.4$ km in Case 8. At 60 min when the cloud is in a most developed stage in Case 8, the maximum vertical velocity is 1.67m/s at $r=1.25$ km and $z=0.6$ km. It is after 110 min that vertical velocity is at its maximum over the center. Vertical velocity exceeds 2.0m/s at $z=0.8$ km in $r \leq 0.75$ km, and the maximum value is 2.53m/s at $r=0$ and $z=0.8$ km at 110 min. As described above, location of the maximum vertical velocity changes greatly as time advances, but the time change in value is rather small till 110 min.

The motion of the circulation described above affects the location where the cloud initially forms and the development of the cloud (see Fig. 2-6). The cloud initially forms not over the center but around $r=2.25$ km and $z=1.0$ km above where larger vertical velocity is recorded at 32 min. The cloud expands horizontally rather than vertically and the inside boundary of the cloud approaches the center. The inside boundary is located at $r=2.0$ km, the outside boundary at $r=2.25$ km, and the cloud top and base are 1.0km, and 0.8km, respectively at 40min. At 80min, the inside boundary is located at $r=0.5$ km. At 110min, the cloud is 2.25km in radius with its top at $z=1.6$ km and base at $z=0.8$ km.

The cloud develops well. The maximum updraft attains 21.0m/s at 143min, and the cloud top reaches $z=9.0$ km. The total amounts of rain are 25.0mm at $r=0$ and 1.1mm at $r=0.75$ km.

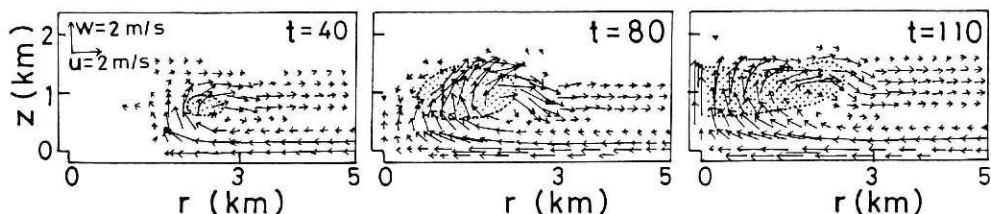


Fig. 2-6 Time changes of air motion and a cloud in Case 12. Air motion is shown by wind vectors and a cloud, by dots. A wind vector is not drawn where both $|u|$ and $|w|$ are less than 0.3m/s.

(4) Comparison of the results of Cases 8 and 14

The vertical grid interval is 200m hitherto in this chapter, while $\Delta z = 100\text{m}$ is usually used when circulation induced by the heat island and others concerning the heat island are numerically studied (e.g., Delage and Taylor, 1970; Sawai, 1978). The effect of the vertical grid interval on the simulation is examined in this section. The vertical grid interval is 100m and the height of integrated domain is 5.5km in Case 14, while the other conditions are the same as those in Case 8.

Time variation of vertical velocity and potential temperature at $r=0$ are shown in Fig. 2-7. Time variations of vertical velocities are larger in Case 14 than in Case 8. There is little difference in potential temperature at $z=0.2\text{km}$ between Cases 8 and 14 after 5 min. Potential temperature is higher in Case 8 before 5 min, because surface temperature directly affects the temperature at $z=0.2\text{km}$ through the diffusion term in Case 8 while not in Case 14. The time variation of the potential temperature at $z=0.8\text{km}$ is larger in Case 14 than in Case 8. The cloud is initiated around $z=0.8\text{km}$ at 25min in Case 14, almost the same position as in Case 8 but earlier than in Case 8 by 2min.

The differences represented are not so essential as to require a modification of the results obtained in sections (1)–(3). However, it is suggested that more noticeable effects of a heat island on the initiation of the cloud and its development than those shown in the previous sections will be demonstrated when $\Delta z = 100\text{m}$.

2-2 Analysis of the Effects of the Heat Island on the Development of a Cloud

The numerical experiments show that the heat island enhances largely the development of a cloud. The effects of the heat island are analytically studied herein.

2-2-1 Effect of the upward motion in the subcloud layer on the development of a cloud

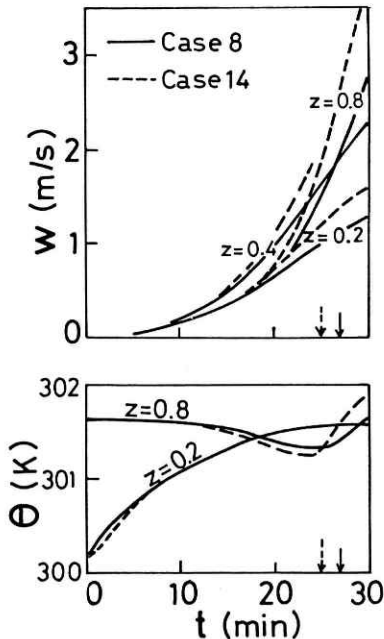


Fig. 2-7 Time variations of vertical velocities and potential temperatures in Cases 8 and 14. The time when a cloud forms is indicated by arrows.

The energy equation of cumulus convection in a closed system can be represented as Eq. (2-19) when both the weight of liquid water and diffusion term can be neglected (see for example, Asai, 1964).

$$\frac{\partial K}{\partial t} = \int \bar{\rho} w g (T_v - \bar{T}_v) / \bar{T}_v dv \quad (2-19)$$

Buoyant force, $g (T_v - \bar{T}_v) / \bar{T}_v$, is written as F_b for abbreviation purposes hereafter.

Work done by buoyant force, F_b , is positive only in the cloud. Thus, Eq. (2-19) may be written as Eq. (2-20), which makes the physical interpretation implied clear. (2-19)

$$\frac{\partial K}{\partial t} = \int_{ic} \bar{\rho} w F_b dv - |\int_{uc} \bar{\rho} w F_b dv| - |\int_o \bar{\rho} w F_b dv| \quad (2-20)$$

The first term on the right-hand side of Eq. (2-20) represents the work of the buoyant force in the cloud, the second term represents the work needed to produce motion in the layer under the cloud base, and the third term represents the work needed to produce motion in other areas such as the compensating downward motion around the cloud (the suffixes ic, uc and o show the integral domains of in-cloud, the layer under the cloud base, and others, respectively).

The Eq. (2-20) clearly shows that work done by the buoyant force in the cloud is the energy source to produce motion under the cloud base and other compensating motions besides increasing kinetic energy. Thus, vertical velocity becomes larger in the cloud when a heat island induces upward motion and the less work is needed for a convective cloud to initiate the upward motion in the subcloud layer. This causes the cloud to develop much better since the energy source of a convective cloud is the heat released by condensation of water vapour which is transported from the subcloud layer. It is upward motion induced by a heat island that enhances the activity of a convective cloud.

2-2-2 Dependence of circulation on a horizontal scale of a heat island

A cloud with a smaller horizontal scale develops less. This is because buoyancy in the cloud is decreased by the entrainment of surrounding air and the entrainment rate is inversely proportional to the radius of the cloud (Squires and Turner, 1962). This holds true for the local circulation induced by the heat island: temperature of an upward current with a smaller radius is lowered more rapidly by entrainment of the surrounding air when upward motion is accelerated.

Then can a larger heat island induce an active local circulation? The numerical experiments show the opposite. A heat island with a smaller radius induces larger vertical velocity at least during early stages and forms a cloud at an earlier time.

Consider a column with radius r_c and height z_c where air starts an upward motion. Let's assume the profile of vertical velocity as Eq. (2-21) after Δt (Sulakvelidze, 1969).

$$w(z) = w_m \left(\frac{z}{z_c} \right) \quad z < z_c. \quad (2-21)$$

This assumes no horizontal variation of vertical velocity, which has been customarily used in studies of cumulus convection (Squires and Turner, 1962; Asai, 1967).

When upward motion is induced, horizontal motion accompanies it. The horizontal velocity is represented as Eq. (2-22) from the continuity equation:

$$u(r) = -\frac{r}{2} \frac{w_m}{z_c} \quad r < r_c. \quad (2-22)$$

Then, the total kinetic energy at Δt is given as

$$K = \int \frac{\bar{\rho}}{2} (u^2 + w^2) dv = \frac{\bar{\rho} w_m^2}{2} \pi r_c^2 z_c \left(\frac{r_c^2}{8 z_c^2} + \frac{1}{3} \right). \quad (2-23)$$

Eq. (2-23) shows that a circulation with a smaller radius has a larger vertical velocity if the amount of energy in a unit volume is the same, i.e., $K/r_c^2 z_c = \text{const.}$ This causes the horizontal velocity to become smaller as the radius of the circulation increases.

The result obtained above is based on the very simple model, but it is essential because upward motion accompanies the horizontal motion whose speed increases proportionally with the increase of upward speed and the radius of the circulation.

From the above it may be concluded that a heat island with a smaller radius may introduce circulation with a larger vertical velocity, but the circulation produced by a heat island with a smaller radius may have a shorter life time because of a rapid decrease of temperature by entrainment.

2-3 Discussion

The following are demonstrated by numerical experiments. (i) Even when the atmosphere is stable, (a) a heat island so modifies the atmosphere that a cloud may develop well over it, and (b) a heat island with a 2°C temperature excess can initiate a cloud which develops well to cause rain. (ii) The initiation of a cloud and its development are directly affected by conditions of a lower layer modified by the heat island, and clouds which form over heat islands with different horizontal scales behave differently.

It is also shown that a heat island affects the development of convection less as the heat island becomes larger over a certain radius. The initial disturbance develops better over the heat island with a radius of 1km than over the heat island with a 12km radius. Likewise, a cloud is formed over a heat island with 18km radius but it does not develop well, and longer time is needed for the cloud to be initiated with increasing the radius of the heat island.

The initial disturbance of a cloud does not develop well in Case 1 where the surface temperature is equal to that at the center of the heat islands in Cases 2-6, where the initial disturbances develop well to cause rain at the surface. Clouds form and develop differently over heat islands with different horizontal scales and different distributions of surface temperature. These show that it is upward motion in the lower layer and not destabilization of static stability that directly enhances the cloud activity over the heat island. The energy equation analysis also indicates that the upward motion induced by the heat island affects and enhances cloud activity.

The comparisons among Cases 2-6 and Cases 7-11 show that a heat island with a smaller radius induces a circulation with larger vertical velocity in early stages and enhances the cloud development less. These are caused by the effects of horizontal motion. An upward motion with a smaller horizontal scale needs less amount of work to induce a compensating horizontal motion. This makes upward velocity larger; While on the other hand, the inflow more notably decreases temperature as the radius of the upward motion is smaller. This leads to a shorter life time of the circulation and a less stimulating effect on cloud development.

When the heat island has a larger radius over a certain value, say 12km, it affects

the cloud development less. This is because velocity of the upward motion induced by a heat island with a larger radius becomes smaller. As described above, a heat island with a smaller radius has less stimulating effects on the cloud development. Thus, a heat island with a certain radius, say 3 to 12km, can affect the development of convective cloud most remarkably.

In this chapter, the term "heat island" is applied to the area where temperature is locally higher noting particular attention to a built-up area. These areas are not very large in size. For example, the Tokyo built-up area is covered by a circle with a 15km radius. Besides, it is rare that a heat island is formed in an entire urban area. The size of the heat island which enhances the activity of cumulus convection most remarkably is comparable to ones of urban areas.

The theoretical conclusion may be made that the heat island in an urban area can be a trigger to initiate a convective cloud and noticeably enhance the cloud activity. The upward motion induced by the heat island directly affects the cloud activity, and it is the upward motion induced by the heat island that enhances the activity of a convective cloud.

3. CASE STUDIES

The effects that a heat island has on convective rainfall will be studied by means of case studies. The occurrences of local heavy rainfalls in the built-up area in Tokyo will be analyzed. Since the theoretical study in the previous section showed that the upward motion induced by the heat island affects the initiation of a convective cloud and cloud activity, the primary concern will be given to the existence of the heat island accompanying the convergence of surface air.

This study contains two cases whose respective maximum 60 minute rainfalls were 96mm and 80mm in the Tokyo built-up area. These were the highest and the second highest values recorded in Tokyo since 1978 when the Bureau of Construction of the Tokyo Metropolitan Government began to publish a yearly record of flood disaster in Tokyo, which contains the maximum values of 60 minute rainfall at every station in the case of large flood disasters.

A record of radar echoes during the time when heavy rainfall occurred in the Tokyo built-up area was available for only one case. The case of 22 July, 1981 will be analyzed to show the heat island effect on the occurrence of heavy rainfall. The other two cases will give evidence in support of the heat island effect.

3-1 *Data Used and Definition of Areas*

The Tokyo Metropolitan Government has more than 50 rain stations and nearly 40 temperature, wind and humidity stations. Data obtained from these stations are used in this study. Data obtained from the Automated Meteorological Data Acquisition System (AMeDAS) points carried out by the Japan Meteorological Agency are also used. Some data obtained by Saitama Prefecture, Kanagawa Prefecture and the Ministry of Construction are also used when necessary.

Figure 3-1 shows the study area, referred to as the Tokyo area. The main built-up area of the central part of Tokyo whose boundary is presented by a bold line in the figure

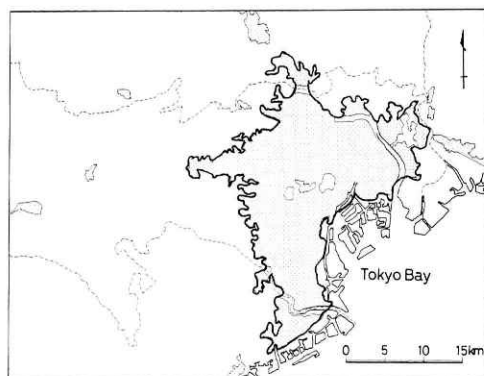


Fig. 3-1 Study area showing the Tokyo built-up area. Dotted areas are built-up areas in 1981 (taken from the topographical map published by the Geographical Survey Institute).

is the Tokyo built-up area in this study.

3-2 The Case of 22 July, 1981

On the evening of 22 July, 1981, a severe local storm occurred in the Tokyo built-up area. It was so severe that great damage was caused. More than 13,000 houses were inundated and traffic was held up due to the failure of electric power supply.

3-2-1 Synoptic conditions

A weak depression with a minimum pressure of 1,008mb was located in the east of Hokkaido. A cold front extended southwestward to the Sanriku and westward to the Noto Peninsula, traversing Honshu Island at the southern part of the Tohoku district at 09 JST on 22 July. Another depression, a weak tropical depression with a minimum pressure of 1,000mb, was located to the east of Hachijo Island. The cold front moved toward the south, and it extended about 200km south of the Tokyo area to the head of the Kii peninsula at 21 JST.

The time-height variations of temperature, wind and water vapour mixing ratio observed at Tateno (see Fig. 3-2) show that the temperature at the surface decreased rapidly on the evening of 22 July, when the cold front passed through the Kanto district. Until then, the lower layer had been warm and moist for more than two days. While at about 500mb height the temperature decreased before 09 JST on 22 July. The atmosphere was vertically unstable in the daytime of 22 July. The Showalter stability index was calculated at -3.4 from the aerological data at 09 JST. It has been known from experiences in the U. S. A. that thunderstorms become increasingly likely as the index values decrease from 0 (Petterssen, 1956). The conditions of the atmosphere were favorable for the occurrence of severe storms. As the time change of the Showalter stability index shows (Fig. 3-2), conditions for a severe storm were also favorable on 20 July. The situation on this day will be referred to in the discussion section.

There were some local heavy rainfalls in the Kanto district on 22 July. According to the AMeDAS data, most of the heavy rainfall occurred independently, and the amount of hourly rainfall was 20-40mm at many points. The amount of 71mm was recorded at Nakaarai in the Tokyo built-up area from 16 to 17 JST. During the next hour from 17 to 18 JST, 73mm was recorded at Haneda, which is located about 20km south of Nakaarai. The distribution of the areas attacked by local heavy rainfalls shows that the

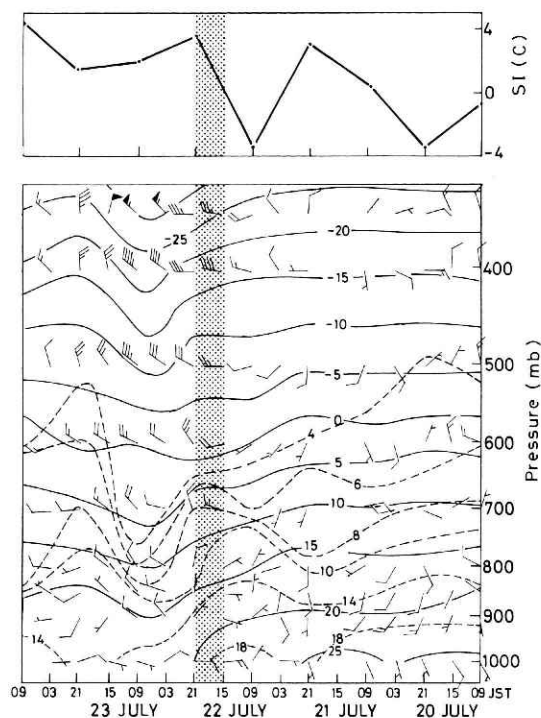


Fig. 3-2 Time-height variations of temperature (solid lines, °C), wind and water vapour mixing ratio (broken lines, g/kg), lower, and time variation of Showalter stability index at Tateno from 20 July to July, 24 1981. The storm analyzed occurred in the shaded time zone.

storm formed and caused the most heavy rainfall in the Tokyo built-up area and moved to the south. The huge amount of rainfall and the movement of the storm were distinguishing features of the storm which occurred in the Tokyo built-up area.

3-2-2 Mesoscale situations in the Tokyo area

Figure 3-3 shows distributions of hourly rainfall in the Tokyo area from 16 to 18

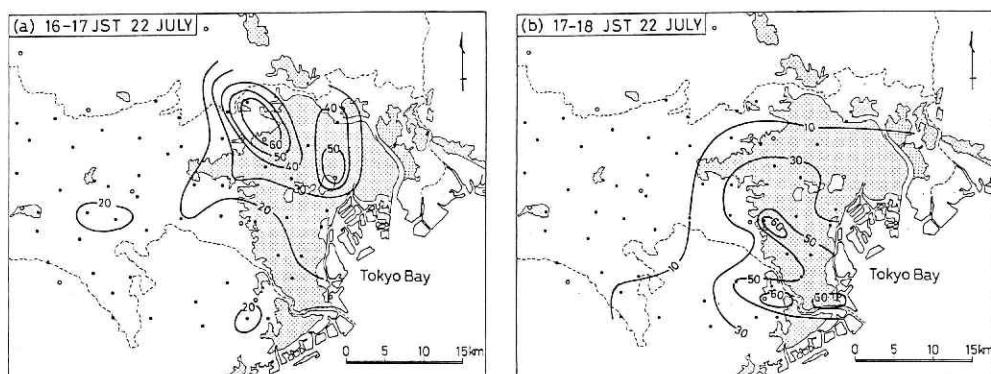


Fig. 3-3 Distributions of hourly rainfall (mm) in the Tokyo area on 22 July, 1981.

JST. In the hour from 16 to 17 JST a heavy rainfall occurred in a small area in the northern part of the Tokyo built-up area. This heavy rainfall was characterized by severity and smallness in the horizontal scale. Several stations recorded more than 30mm and the maximum was 71mm recorded at Nakaarai from 16 to 17 JST. The area which received over 30mm was very small and could be approximated by a circle with a radius of 10km.

Rainfall amounted to 73mm in the hour from 17 JST at Haneda, which had recorded only 14mm in the one hour prior to 17 JST, while the hourly rainfall was 14mm at Nakaarai. The area which experienced heavy rainfall from 17 JST was located in the southern part of the Tokyo built-up area. The storm moved southward and continued to produce heavy rainfall. The built-up area received heavy rainfall of more than 40mm during the 2 hours after 16 JST.

Figure 3-4 shows the fields of surface temperature and surface wind at 15, 16 and 17 JST. In the morning and the afternoon of 22 July, the temperature was higher in the built-up area than in the surroundings by about 2°C , and there was a vague heat island present with a few peaks. At 15 JST, an obvious heat island formed in the northern part of the Tokyo built-up area. Temperature was 33°C at the center of the heat island and was higher than that in the surroundings by about 2°C . (This is referred to as heat island "A", hereafter.) There was a small heat island present as well. It existed in the southern part of the Tokyo built-up area. The temperature was 31°C and was higher than in the surroundings by 1°C . (This is referred to as a heat island "B", hereafter.)

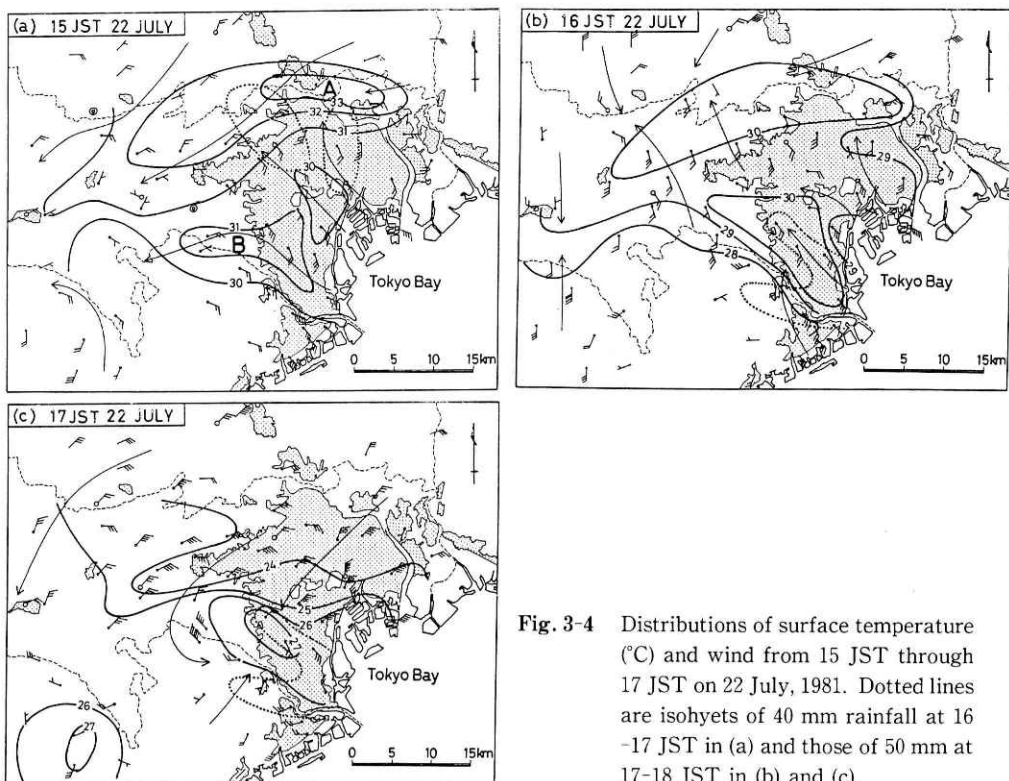


Fig. 3-4 Distributions of surface temperature ($^{\circ}\text{C}$) and wind from 15 JST through 17 JST on 22 July, 1981. Dotted lines are isohyets of 40 mm rainfall at 16-17 JST in (a) and those of 50 mm at 17-18 JST in (b) and (c).

The sizes of heat islands "A" and "B" are not very large nor very small. Areas where the temperature was over 33°C in "A" or over 31°C in "B" cover about the size of $15 \times 3 \text{ km}^2$. The heat islands had a suitable size for remarkably enhancing convective activity, which is shown in the numerical study in Chapter 2.

As a whole the wind was weak in the Tokyo area until 15 JST. At 15 JST, there were two systems of winds on a rather large scale. One system was a northeasterly wind, predominating in the northwest part of the Tokyo area. This wind system was evident from about noon. The other was a flow which blew landward from the Tokyo Bay. This was a sea breeze. Besides these two systems of winds, another air flow was recognizable although it was very local. There were inflows toward the center of heat island "A" around the southern part of the heat island where the temperature gradient was large. A high speed of 4 m/s was recorded at a few points there. There was also a large convergence of surface wind over heat island "A" (see Fig. 3-5).

The area where initial heavy rainfall occurred was the central part of heat island "A" and the vicinity immediately to the south of it. It began to rain heavily at 16 JST, one hour after the obvious heat island "A" had formed.

Heat island "B" was more remarkable at 16 JST than at 15 JST. The temperature was over 30°C at the heat island, while it was $29\text{--}30^{\circ}\text{C}$ in the central part of the Tokyo area and less than 28°C in the southern part. Thus, heat island "B" had a temperature excess of 2°C . As for the wind field, it was not obvious whether there was a convergence of the surface wind around "B" while there was still a remarkable one around "A" (see

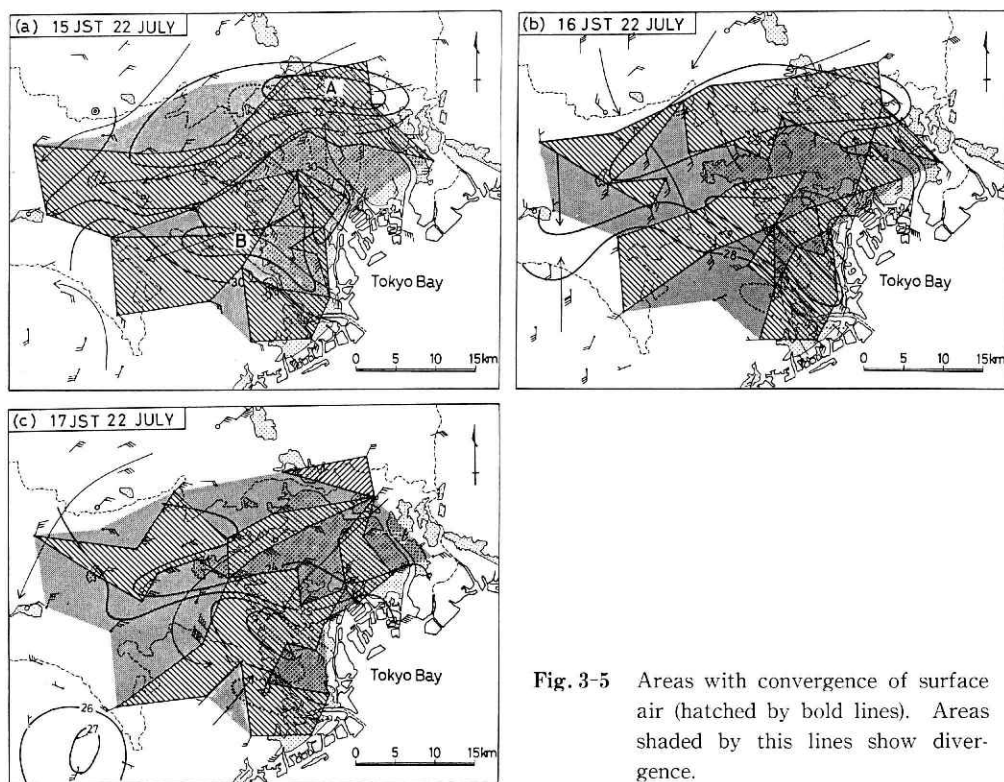


Fig. 3-5 Areas with convergence of surface air (hatched by bold lines). Areas shaded by this lines show divergence.

Fig. 3-5 (b)). However, an inflow toward heat island "B" was observed at a few points where the temperature gradients were the largest.

At 17 JST, heat island "B" became more noticeable and there was an obvious convergence toward heat island "B". Temperature in heat island "B" decreased to 26–27°C, while it decreased below 24°C in the northern half of the Tokyo built-up area. This was caused by the cold downdraft which had been initiated by the heavy rainfall during 16–17 JST. The convergence was also enhanced by a divergence of air which, accompanied with the downdraft, took place in the immediate vicinity of heat island "B". It was in heat island "B" that a heavy rainfall occurred during the one hour from 17 JST.

3-2-3 Behaviour of radar echoes

The Tokyo Meteorological Observatory recorded radar echoes with an interval of less than five minutes starting before 15 JST. There were many radar echoes in the area of 100km from the observatory, but there was no echo in the Tokyo built-up area before 15:20 JST.

Figure 3-6 shows the time variation of the horizontal distribution of radar echoes in and around the Tokyo built-up area during the two hours from 15:30, thirty minutes before the occurrence of heavy rainfall. A small echo which appeared in the south of the eastern edge of heat island "A" before 15:30 grew over the area, and the echo had covered the eastern part of heat island "A" by 16:08.

Over the western part of heat island "A" two echoes had formed also by 16:08. They began over the area where the gradient of the surface temperature was the largest in the western part of the heat island at 15 JST.

Between 16:08 and 16:23, there were rapid expansions of the echoes to the south. At 16:16 the echoes covered almost the entire area that received heavy rainfall during the one hour from 16 JST. At 16:23, the four echoes of 16:08 combined and formed one echo. It covered the northern part of the Tokyo built-up area.

By 16:58, the echo had changed its shape entirely. The echo which existed over the south of the boundary between Metropolitan Tokyo and Kangawa Prefecture at 16:23 had dissipated by this time. The echo had an axis extending southwest and northeast and moved southward. At 17:21 the entire heat island "B" was covered by the echo. It may be worthy to note that an echo which had been travelling southeastward and was in a dissipating stage combined with the echo concerned at the northern edge of the echo.

There were three areas where extremely heavy rainfall occurred. Two of them were located in and in the vicinity of heat island "A" and are referred to as Area No. 1 for the area in the eastern part and Area No. 2 for the one in the western part. The other area was located in and in the vicinity of heat island "B". This is referred to as Area No. 3 (see Fig. 3-6).

The behaviour of the radar echoes shows the following characteristics in regard to the occurrence of the heavy rainfall in the three areas.

- (a) The storm which attacked Area No.1 was first observed as a small echo over the vicinity of the eastern part of heat island "A". Because the echo expanded and heavy rainfall occurred only in and in the vicinity of heat island "A", it is considered that the heat island enhanced the convective activity and caused heavy rainfall in Area No. 1.

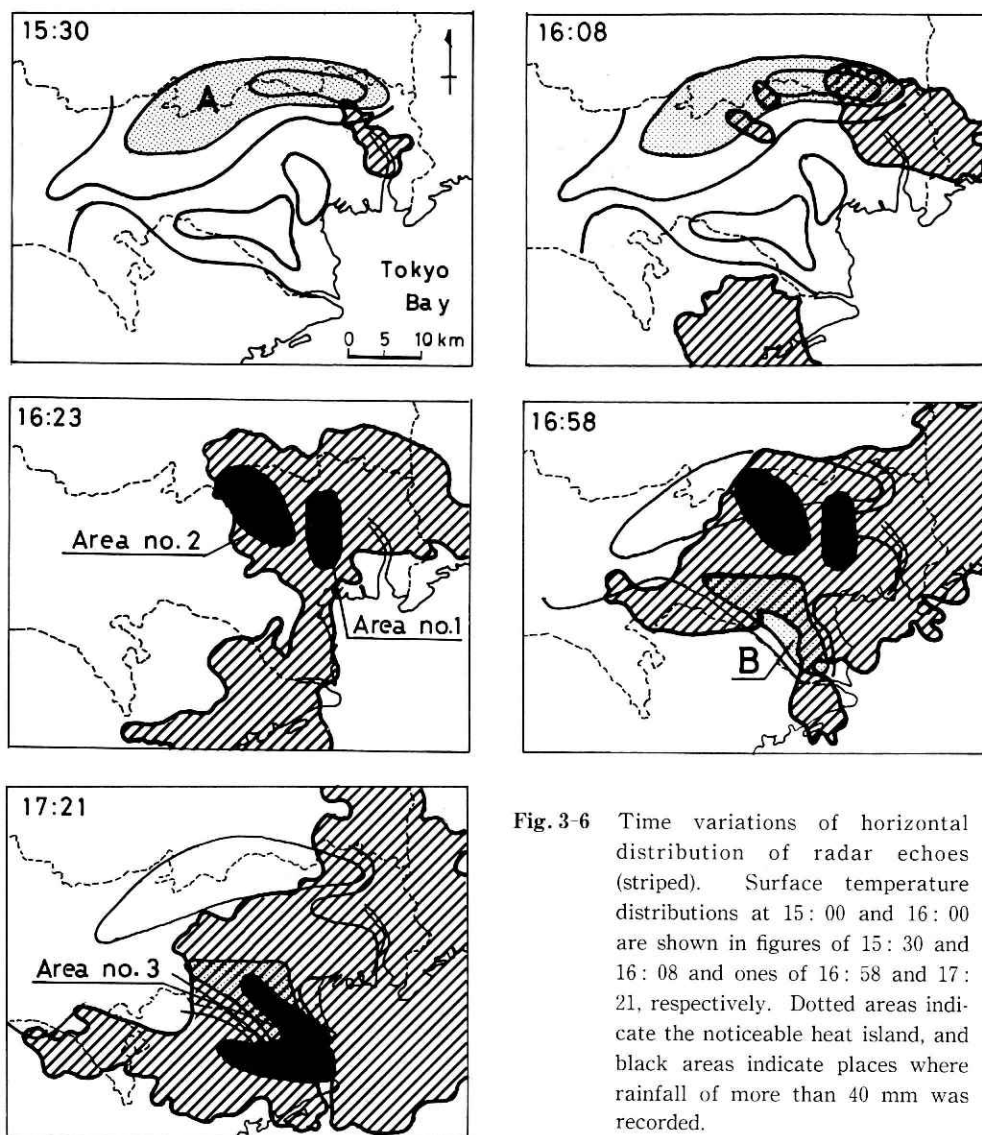


Fig.3-6 Time variations of horizontal distribution of radar echoes (striped). Surface temperature distributions at 15:00 and 16:00 are shown in figures of 15:30 and 16:08 and ones of 16:58 and 17:21, respectively. Dotted areas indicate the noticeable heat island, and black areas indicate places where rainfall of more than 40 mm was recorded.

- (b) The storm that hit Area No. 2 was first detected as two small echoes which appeared over the western part of heat island "A". It is clearly shown that the storm was formed over heat island "A".
- (c) The heavy rainfall in Area No. 3 was caused by a small part of the large echo. The part travelled over heat island "B".

3-3 The Case of 14 July, 1985

On 14 July, 1985 when the Bai-u season was over in the Tokai area, the maximum temperature measured at the Tokyo Meteorological Observatory was 32.2°C. It was the third tropical hot day in July. Heavy rainfalls occurred in the southern part of the Kanto

district in the late afternoon. A severe local storm occurred around the southeastern part of the Tokyo built-up area and caused great flood damage. One life was lost and more than 2,200 houses were inundated

3-3-1 Synoptic conditions

A depression with a minimum pressure of 992mb was located in the Japan Sea close to Aomori Prefecture, and it moved eastward at 09 JST on 14 July. A cold front extended southeastward from the depression to about 200km offshore of the Sanriku and southwestward to the Kii peninsula along the coastline in Kanagawa Prefecture and Shizuoka Prefecture. The cold front also moved eastward and extended into the Pacific Ocean far from the northern part of Honshu at 21 JST.

Figure 3-7 shows time-height variations of temperature, wind and water vapour mixing ratio observed at Tateno in the Kanto district. Warm air existed in the layer below the 600mb height from 13 July to 14 July. On 15 July, the Kanto district was covered by a cold and dry air mass. The minimum relative humidity was 32% at the Tokyo Meteorological Observatory, which was the lowest measurement for July. The cold air first appeared in the upper layer. The temperature at the 500mb height decreased from -3.8°C at 09 JST to -9.9°C at 21 JST on 14 July.

The vertical stability changed for the worse in the daytime of 14 July when warm wet air existed in the lower layer and cold air entered in the upper layer. The Showalter stability index was calculated at 1.8 from the aerological data at 09 JST and -1.8 at 21 JST. The time change of Showalter stability index shows that the atmospheric conditions were most favorable for the occurrence of thunderstorms during the 5 days from 12 July to 16 (see Fig. 3-7).

Local heavy rainfall occurred in some places in the Kanto district on the afternoon of 14 July according to the AMeDAS data. There were five stations where more than 30mm of hourly rainfall was recorded; three of them were located in the Tokyo built-up area. The highest value was 50mm at Nakaarai in the built-up area. The local storm that occurred in the Tokyo area was the most severe among the storms which occurred on 14 July. It is also shown that the storm moved southeast.

3-3-2 Mesoscale situation in the Tokyo area

Mesoscale distributions of an hourly rainfall of more than 20mm in the Tokyo area from 17 to 19 JST are shown in Fig. 3-8. A heavy rainfall with a peak value exceeding 40mm in an hour occurred in only a very small area from 17 JST. The rainfall was so localized that AMeDAS stations did not observe it. Only 1mm was recorded at the Hachioji AMeDAS station, which is less than 10km from the center of the heavy rainfall area.

One hour after the occurrence of the heavy rainfall, a severe local storm occurred in a much wider area. The area had a rather oblong shape and the length of the longer side was nearly 40km. The peak value of rainfall was recorded in the central part of the area. The value was 77mm at Koudaibashi, where 96mm was recorded during 60 minutes. It began to rain there after 18:30 JST, while it began to rain before 18:20 in the northern part of the area. It rained 77mm at Koudaibashi in a 30 minute time period. It should be noted that the peak value of hourly rainfall was recorded at Koudaibashi where it

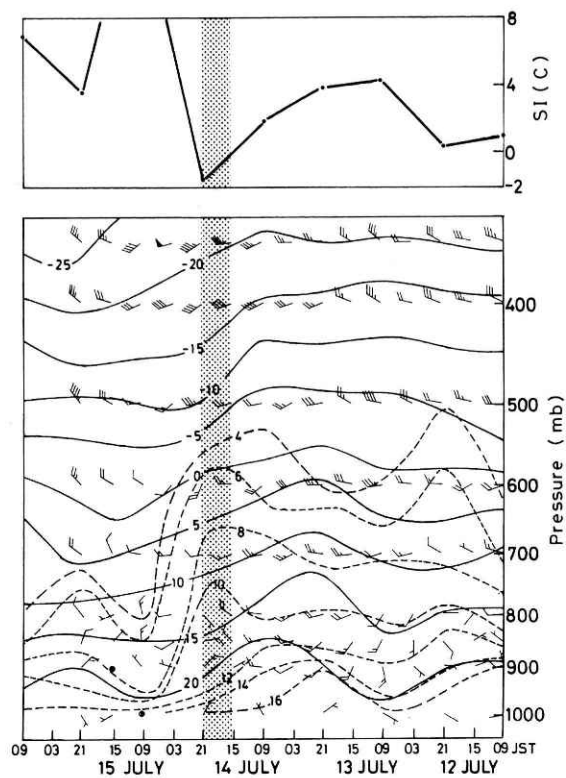


Fig. 3-7 Time-height variations of temperature (solid lines, in unit of $^{\circ}\text{C}$), wind and water vapour mixing ratio (broken lines, g/kg), lower, and time variation of Showalter stability index, upper, at Tateno from 12 July to 16 July, 1985. The severe local storm analyzed occurred in the shaded time zone.

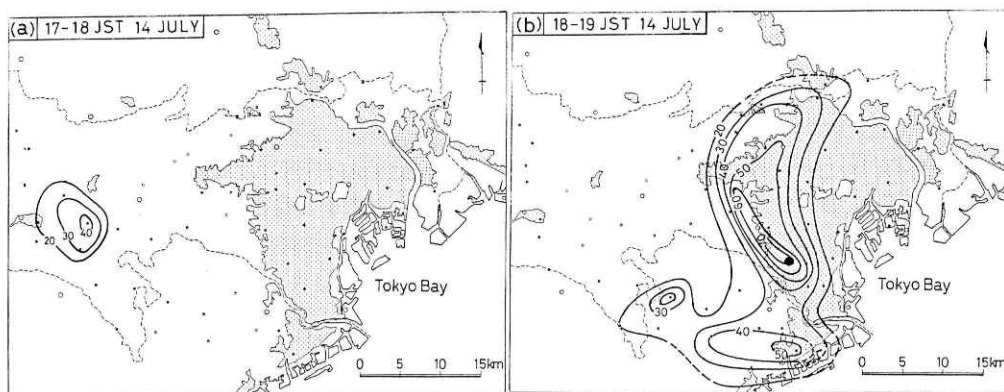


Fig. 3-8 Distributions of hourly rainfall (mm) in the Tokyo area on 14 July, 1985.

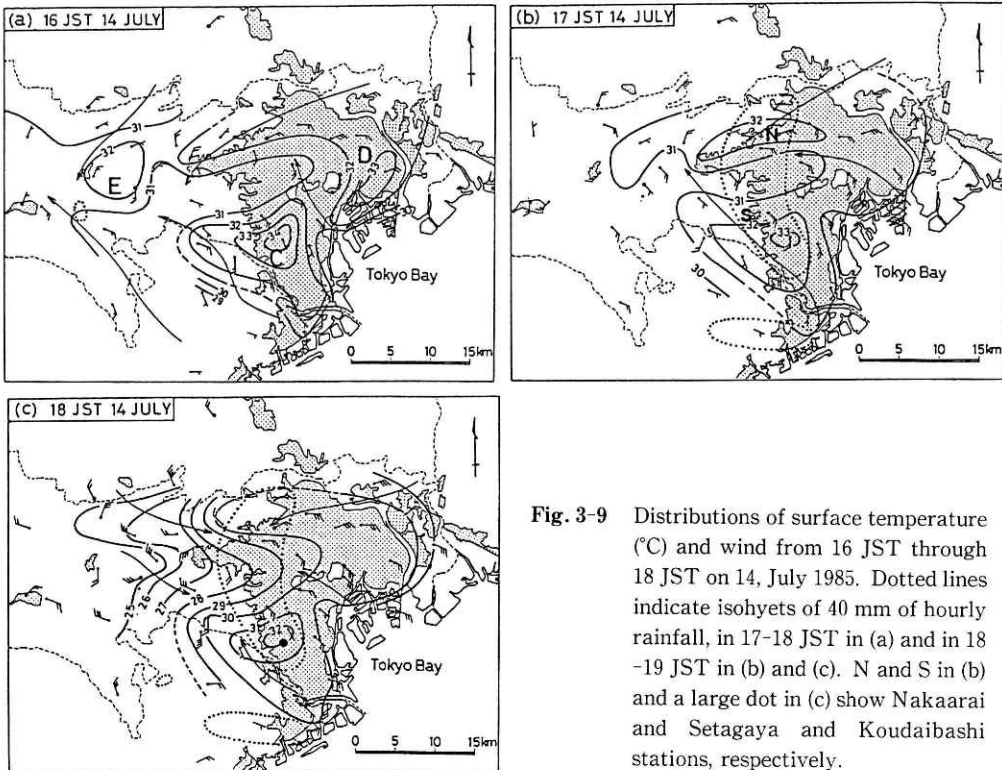


Fig. 3-9 Distributions of surface temperature ($^{\circ}\text{C}$) and wind from 16 JST through 18 JST on 14, July 1985. Dotted lines indicate isohyets of 40 mm of hourly rainfall, in 17-18 JST in (a) and in 18-19 JST in (b) and (c). N and S in (b) and a large dot in (c) show Nakaarai and Setagaya and Koudaibashi stations, respectively.

started to rain later than in the northern part of the area which received heavy rain.

Surface temperature distribution at 16 JST shows there were three areas where the temperature was locally high (see Fig. 3-9(a)). The most noticeably warm area was an area located in the southeastern part of the Tokyo built-up area, and the temperature was higher by 4°C at its center than in the surrounding area. The other two were not so noticeable, because they were small in area and small in temperature difference. These heat islands are referred to as heat island "C", heat island "D", and heat island "E", as denoted in the figure, respectively.

The wind field shows that there was a convergence of air (see also Fig. 3-10(a)). A horizontal convergence of air took place around heat island "E", which was located in the outside of the Tokyo built-up area. In the immediate vicinity of heat island "E", it began to rain heavily one hour later at 17 JST.

At 17 JST, the heat islands "C" and "D" still existed (Fig. 3-9(b)). Temperature distribution shows that the center of heat island "D" had moved to an area around Nakaarai, and the area was almost 15 km by 3 km. This is equal to the sizes of the centers of the heat islands "A" and "B" in the case of 22 July, 1981.

An easterly wind was dominant and its speed exceeded 2 m/s at many points on the east side of the Nakaarai-Setagaya line, while there were only a few points where the wind speed exceeded 2 m/s on the west side of the line. There was a convergence along the line connecting Nakaarai and Setagaya (Fig. 3-10(b)).

At 18 JST, two heat islands were still present in the built-up area (Fig. 3-9(c)). Heat

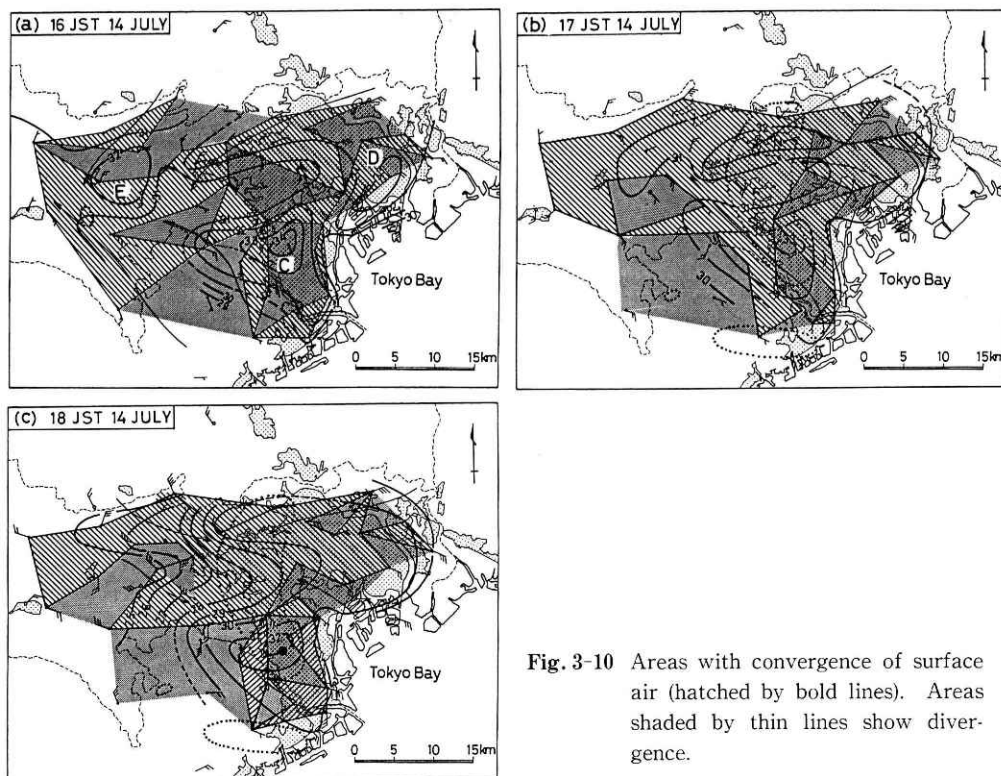


Fig. 3-10 Areas with convergence of surface air (hatched by bold lines). Areas shaded by thin lines show divergence.

island "C" continued and created the center of the large heat island. When looking at a mesoscale view, it may be said that heat island "C" existed noticeably in the southeastern part of the Tokyo built-up area. There was a large and obvious convergence of air in the vicinity of the heat island.

After 10 minutes, a heavy rain began to fall in the area of the northern part of the heat island, and heavier rain began to fall in and around the southern part of heat island "C" 30 minutes later. The Koudaibashi raingauge station, which recorded as much as 77mm during a 30 minute period, was located in the center of heat island "C".

3-4 The Case of 15 May, 1979

A depression moved very slowly to the east near the Pacific Ocean side of Honshu from 14 May to 15 May, 1979. It continued to rain for 30 hours in the Tokyo area from the early morning of 14 May, and the Tokyo built-up area experienced heavy rainfall of more than 30mm during one hour from 02 JST on 15 May. After a fair amount of rain had fallen, flood disasters occurred. More than 1,900 houses were inundated. The amount of 30mm of hourly rainfall was very great for this time of year. The highest value recorded since 1886 of hourly precipitation measured at the Tokyo Meteorological Observatory for the month of May had been 35.5mm.

3-4-1 Synoptic conditions

A depression which was moving slowly eastward was located around the Osaka

Prefecture with a minimum pressure of 994mb at 15 JST on 14 May. This moved toward Mie Prefecture at 21 JST on 14 May and near the Izu peninsula at 03 JST on 15 May. It began to rain in the Tokyo area from about 04 JST on 14 May. The total amount reached over 60mm by 24 JST of 14 May.

The time-height variations of temperature, wind and water vapour mixing ratio are shown in Fig. 3-11. It is shown that moist air began to advect to the Kanto District from the south in the lower layer from the evening of 13 May. The atmosphere was very dry, especially in the lower layer on 12 and 13 May, and changed to a moist condition from the evening of 13 May. The temperature increased remarkably in the lower layer during the period from the morning of 14 May to daybreak of 15 May. For example, it increased at 800mb height from 2.7°C at 09 JST to 4.2°C at 21 JST on 14 May and to 8.5°C at 09 JST on 15 May. On the other hand, the temperature decreased rapidly at the upper levels from 21 JST on 14 May to 09 JST on 15 May. As a result, the atmosphere became favorable for the occurrence of convective storms during the 12 hour period from 21 JST on 14 May to 09 JST on 15 May. The Showalter stability index decreased from 8.9 at 21 JST to 0.4 at 09 JST during the same time period.

Rain began to fall in the Kanto District from the early morning of 14 May. Heavy rainfall of more than 10mm an hour was recorded at many places in the Kanto Plain

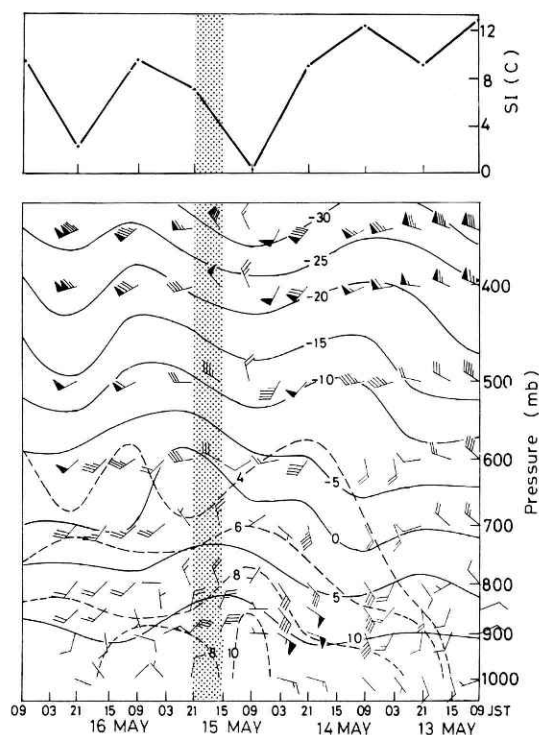


Fig. 3-11 Time-height variations of temperature (solid lines, °C), wind and water vapour mixing ratio (broken lines, g/kg), lower, and time variation of Showalter stability index, upper, at Tateno from 13 May to 17 May, 1979. The storm analyzed occurred in the shaded time zone.

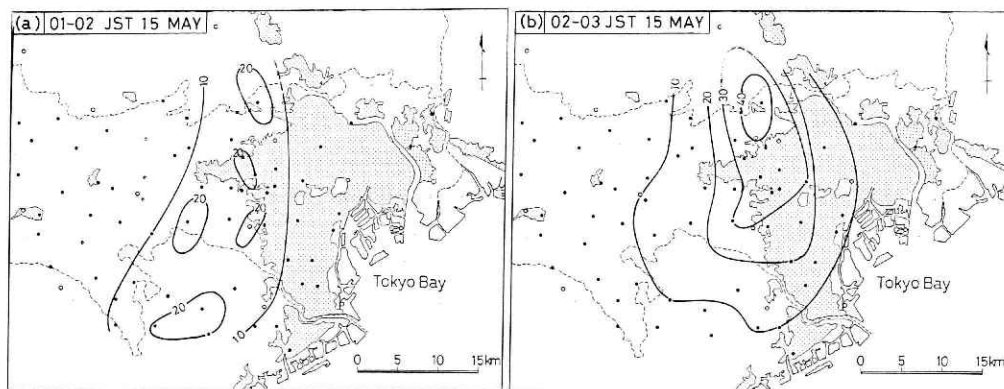


Fig. 3-12 Distribution of hourly rainfall (mm) in the Tokyo area on 15 May, 1979.

from 20 JST on 14 May to 04 JST on 15 May.

The movement of the area of heavy rainfall became rather complicated after 01 JST on 15 May. Around the southern end of the Abukuma mountainous region heavy rain continued to fall. This was considered to be an indication that the heavy rainfall was caused by the enhancement of rainfall by an orographic effect. Around the Tokyo built-up area, a heavy rain also continued to fall for two hours. Hourly rainfalls of more than 20mm were recorded at Setagaya at 02 and 03 JST, and that of 34mm was recorded at Nakaarai at 03 JST on 15 May. Both stations are located in the Tokyo built-up area. It is hard to explain from the synoptic conditions what caused the heavy rain to continue in and around the Tokyo built-up area.

3-4-2 Mesoscale situations in the Tokyo area

Mesoscale distributions of hourly rainfall of more than 10mm in the Tokyo area from 01 to 03 JST are shown in Fig. 3-12. In the one hour prior to 02 JST, several stations recorded more than 20mm of rainfall. In the next hour, until 03 JST, heavy rainfall was recorded in a wide area with a peak value of 45mm at Akatsuka near Nakaarai. The area extended in the directions north and south in and around the western part of the Tokyo built-up area. Afterwards, heavy rainfall was not recorded at any station in the Tokyo area.

The time change of temperature distribution showed that the temperature in the built-up area was higher than in the surroundings by 2°C at its maximum through the afternoon and the evening of 14 May. The temperature increased in the built-up area as time advanced until midnight when warm air advected from the south, changing from 14.9°C at 23 JST to 16.0°C at 24 JST, to 16.8°C at 01 JST, and to 16.7°C at 02 JST at the Tokyo Meteorological Observatory. After 02 JST, it gradually decreased to 13.9°C at 08 JST on 15 May. The heat island became remarkable about midnight on 14 May as shown in Fig. 3-13. Isotherms ran more densely near the built-up area and a heat island with a few peaks formed. The temperature exceeded 15°C in many points in the built-up area and several points recorded temperatures above 16°C at 24 JST. The wind field shows that there was a convergence around one of the peaks of the heat island (Fig. 3-14). The region where heavy rainfall occurred one hour later extended northward and southward,

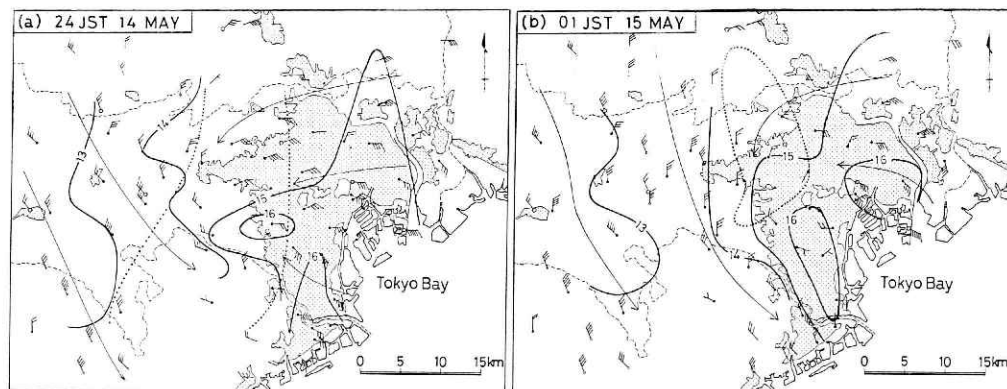


Fig. 3-13 Distributions of surface temperature ($^{\circ}\text{C}$) and wind at 24 JST on 14 May and 01 JST on 15 May, 1979. Dotted lines are isohyets of 10 mm rainfall in 01-02 JST in (a) and 30 mm rainfall in 02-03 JST in (b), respectively.

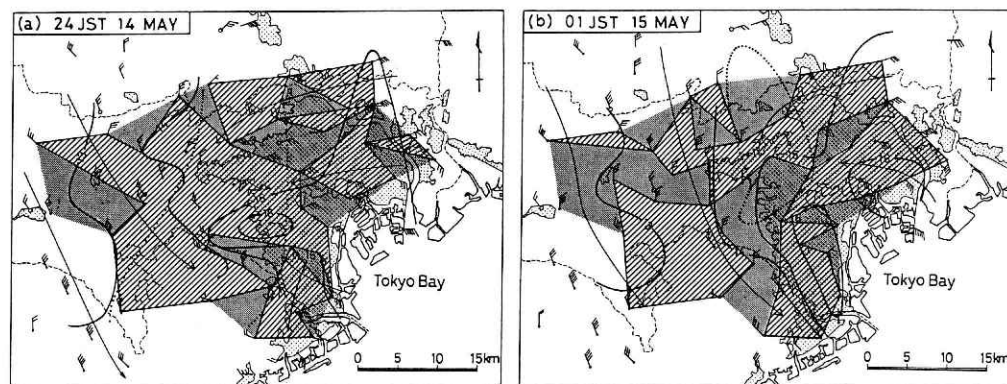


Fig. 3-14 Areas with convergence of surface air (hatched by bold lines). Areas shaded by thin lines show divergence.

centering around this area.

At 01JST, the temperature exceeded 16°C at many points in the built-up area and the region with a temperature above 15°C expanded its width. Surface flow converged towards the heat island. In the western part and northwestern vicinity of the heat island, it rained much more heavily one hour later. The center of the heavy rainfall was located about 20km from the center of the heat island. The direction from the center of the heat island to the center of the heavy rainfall coincided with the directions of the wind in the lower layer below the 700mb level (see Fig. 3-11).

3-5 Discussion

The heavy rainfalls that were analyzed in this section are characterized by the following three features: (i) they were very severe and local, and their peak values of rain were unusually large; (ii) the storms which caused them were suggested to cause continuous heavy rains for more than one hour, though this did not happen in other places

in the Kanto District, except near the mountainous region on 15 May, 1979; (iii) these unusually heavy rainfalls occurred in and in the vicinity of where the obvious heat islands had formed in the Tokyo built-up area.

The analysis of radar echoes in the case of 22 July, 1981 showed that there were two echoes which first appeared over the heat island and a large echo covered the Tokyo built-up area. but heavy rainfalls were recorded only in small areas in and in the vicinity of the heat island. These findings indicate that the heat island formed convective clouds and enhanced convective activity to cause heavy rainfall, as was numerically shown in the previous section.

Heavy rainfall was also recorded in and in the vicinity of the heat island in the case of 14 July, 1985. The general wind was weak on that day. These situations are similar to those of the case of 22 July, 1981. It was about one hour or so after the formation of the heat island accompanied by the convergence of surface flow that very heavy rain occurred in all cases. These findings support that the heat islands had an effect on the occurrence of all heavy rainfalls studied.

A few case studies showed that the heat island had formed prior to the occurrence of heavy rainfall in London (Parry, 1956; Atkinson, 1971) and Washington D.C. (Harnack and Landsberg, 1975), and it was suggested that the heat inland aggravated convective storms. All cases studied here show the same antecedent meteorological conditions as the ones previously studied.

Vertical conditions of the atmosphere were favorable for the occurrence of severe local storms on 20 July, 1981. Actually, a few thunderstorms occurred in the Kanto District; a hailstorm occurred at Chichibu in the mountainous region of Saitama Prefecture. But rainfall of more than 10mm was not recorded in the Tokyo area. A heat island was not seen in the Tokyo built-up area on that day either. On the other hand, an obvious heat island, i.e., heat island "C", formed at 16 JST on 14 July, 1985, but it began to rain heavily at another place after 17 JST on the same day. At that time heat islaon "C" was not accompanied by the convergence of surface flow.

The temperature distributions showed a resemblance in pattern between the ones on 22 July, 1981 and on 14 July, 1985. The temperature was locally high in the northern part and the southern part of the built-up area. This bears a resemblance to the distribution of the mean maximum temperature in August studied by Kawamura (1977). On 15 May, 1979, the temperature was high in the entire built-up area.

According to Yoshino (1975), sea winds invade as far as 6-7km inward and a calm zone is formed there. The situation of this windless zone varies a little according to the direction and velocity of the prevailing wind. Because sea winds develop best at high noon and prevailing winds were weak on both 14 July, 1981 and 22 July, 1985, the sea breeze may play an important role in the formation of the heat island around the edge of the built-up area.

The case study shows the following: the heavy rainfalls which had unusually large peak amounts and gave rise to great flood damage were caused by the heat island. A heat island can not always bring about a local circulaoion to initiate a local storm, but it can be an important causative factor in the occurrence of a severe local storm in the Tokyo buiqt-up area.

There was a case when the convergence was enhanced by a downdraft caused by

heavy rainfall. Thus, it is suggested that the interaction between the heat inland and a storm affects the development of the storm. This is considered to be another effect of the heat island on the convective phenomenon with precipitation.

4. STATISTICAL STUDY

It was shown in the previous sections that a heat island could affect the development of convective phenomena with precipitation. This chapter will statistically deal with the magnitude of the heat island effect on the occurrence of strong convective rainfall in Tokyo. First, it will be shown that a heat island has a considerable effect on the occurrence of heavy precipitation in August. Second, conditions of when only the Tokyo built-up area had local strong rainfall will be elucidated, and the number of days with strong rainfall in the built-up area and the number of days when conditions were favorable for the occurrence of strong precipitation will be studied. The comparison of these two numbers will give the estimate of the possibility for the heat island to cause strong rainfall.

Japan is a mountainous country, and there is a lot of precipitation caused by the Bai-u front, typhoons and other disturbances. Amounts of precipitation vary widely according to the courses of these disturbances because of the topographic effects on precipitation, noting generally more precipitation in mountainous areas. This may be why an urban maximum in the total amount of precipitation is not usually noted in Japan, although an increase in the number of days with drizzle has been shown in many cities (Yoshino, 1957, 1977).

The distribution of the average total monthly precipitation in August is noted. The total monthly precipitation increases from 150 mm in the eastern area around Tokyo Bay to 300 mm in the western mountainous areas. The monthly total is 150-200 mm in the built-up area.

4-1 *Increase in the Number of Days with Heavy Precipitation in the Tokyo built-up Area.*

Section 4-1 will show that in recent years heavy precipitation has occurred more often in the Tokyo built-up area in August than before. It will also be shown that this is closely related to the frequency of the appearance of a noticeable heat island.

4-1-1 Data used

In this section, the number of days with precipitation in August is analyzed. Weather in August is characterized by relatively high humidity and the occurrence of thunderstorms. Occasionally, a typhoon occurs in Japan, and this causes high precipitation with a distribution usually showing a marked topographic effect. The urban effects on precipitation are noticeable when it is calm and are not so when synoptic conditions are stormy (Yoshino, 1977). Thus, data are excluded from this study on days when a typhoon or a tropical depression influenced the weather in the Tokyo metropolitan area (daily amounts of precipitation at representative stations on these days are tabulated in Appendix B).

The Japan Meteorological Agency had auxiliary stations until 1977 when the

Automated Meteorological Data Acquisition System (AMeDAS) came into operation. The discussions in this section are based on data observed at the auxiliary stations in and around the Tokyo area defined in section 3 from 1954 to 1976. These data are given in the monthly reports of weather published by local meteorological offices such as the "Tokyo-to Kishi Geppo". The locations of the auxiliary stations are shown in Fig. 4-1. There were more than 40 stations in the study area.

The AMeDAS data are used to study the situation during the ten years after 1977. The number of AMeDAS stations in the study area is 18. Because of the type of raingauge used and the difference of the method of observation and station locations from the time up to 1976 and after 1977, analysis will first be made on the data till 1976. Tokyo greatly developed by 1976 and had become one of the largest cities in the world.

4-1-2 Distributions of daily precipitation in two five-year periods : 1972-76 and 1954-58

Comparisons are made between the distributions of the number of days with a specified amount of precipitation in the built-up area and those in the surroundings. The number of days with a specified amount of precipitation is the total of the figures at three stations from both the built-up area and its surroundings. The three urban stations are Tokyo, Shinjuku and Setagaya, and the suburban stations are Murayama, Hachioji and Machida, respectively (see Fig. 4-1 for their locations). These stations began observations before 1955, except Shinjuku, which began observations in 1965 when Yodobashi ceased observations. The distance between the Yodobashi station and the Shinjuku station is about 1.8 km, and tests authorized by the Japan Meteorological Agency have shown that the shift of the observation station has not affected the continuity of the records of annual total precipitation and annual maximum daily precipitation. Thus, the two series of data observed at Shinjuku and Yodobashi are treated as one set of successive chronological data.

Figure 4-2 shows distribution of precipitation over a five year period from 1972 to 1976. The total number of days with 1 mm or more is larger in the built-up area than in the surroundings every year, while larger amounts of precipitation, say more than 21 or 31 mm, are recorded more often in the stations in the built-up area in 1972, 1974 and

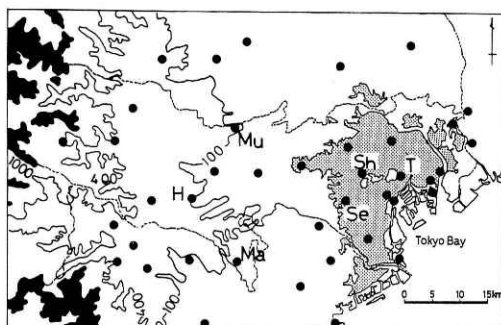


Fig. 4-1 Study area showing precipitation stations (dots), the Tokyo built-up area (dotted) and topography. T, Sh and Se indicate locations of Tokyo, Shinjuku and Setagaya in the Tokyo built-up area, and Mu, H and Ma indicate locations of Murayama, Hachioji and Machida in the surroundings.

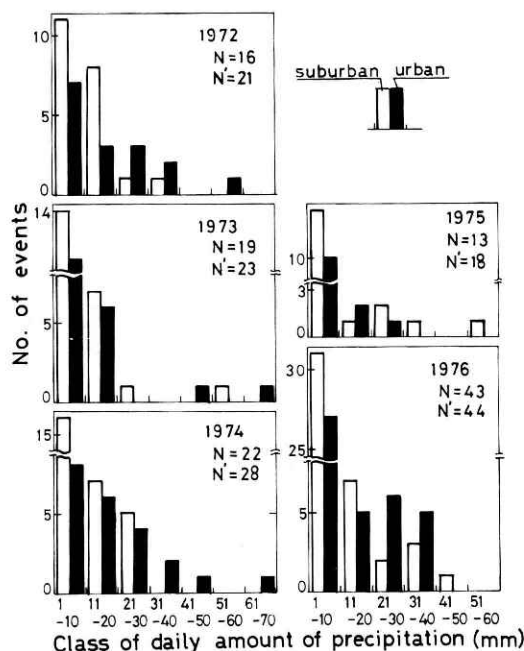


Fig. 4-2 Frequencies of occurrence of the daily amount of precipitation in August from 1972 to 1976. The ordinates are the total number of events at the three stations in the urban suburban areas. N indicates the total number of events at the three stations in the urban/area, and N' at the stations in the surroundings.

1976. Only in 1975 was a larger amount of precipitation recorded at stations in the surroundings.

As can be seen from the distributions, the total monthly precipitation was small in 1973 and 1975, at 40% of the normal value in 1973 and 20% in 1975. In these two years, higher precipitation in the built-up area is either not clear or absent.

The tendency shown in Fig. 4-2 is not seen in the five years from 1954 to 1958 (see Fig. 4-3). Observations were missed on 10 days in 1954 and 20 days in 1956 at a station in the surroundings. The 10 days in 1954 when observations were missed at Machida included two days when high precipitation was recorded at stations in both the built-up area and surroundings. Amounts of 93 and 25 mm were recorded at the nearest station to Machida. Although there are two years without complete data for the surrounding areas, no distribution in Fig. 4-3 shows a tendency for a larger amount of precipitation to be recorded more often in the built-up area.

The change in the number of days with high precipitation is studied in the following section. Hereafter, precipitation of not less than 31 mm is called heavy precipitation, and the number of day with heavy precipitation is investigated.

4-1-3 Change in number of days with heavy precipitation

Figure 4-4 shows the change in the number of days with heavy precipitation in the urban and suburban areas every five years during the 1957-76 period. The number of days with heavy precipitation for each area is the total of the numbers at the same three

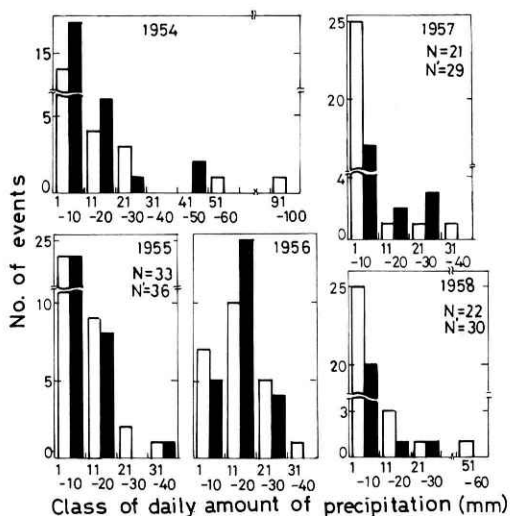


Fig. 4-3 Same as Fig. 4-2, but from 1954 to 1958.

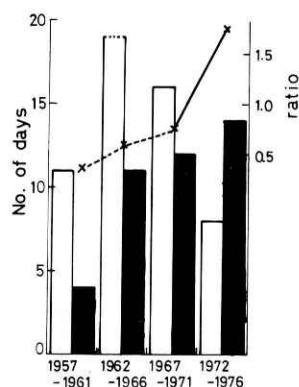


Fig. 4-4 Variations in the total number of days with precipitation of not less than 31 mm every five years. Black indicates the three stations in the built-up area, and white the three stations in the surroundings. The line shows the variation of the ration (total number of days in the built-up area)/(total number of days in the surroundings).

stations as identified in Section 4-1-2.

For the first preiod 1957-61, the number of days with heavy precipitation was only 4 days in the urban area, less than half of the 11 days recorded in the suburbs. For the second period, 1962-66, observations were missed at Hachioji in 1965 and 1966. Distri-butions of daily precipitation around Hachioji suggest that there were two or three days with heavy precipitation at Hachioji during these two years. The number of days with heavy precipitation may be considered to be about 21 in the suburbs for the second period. It was 11 in the urban area, about half. This ratio shows that there is little difference in the occurrence of heavy precipitation between the first period and the second period.

The number of days with heavy precipitation was 12 in the urban area and 16 in the suburbs for the period 1967-71. The number was larger in the urban area than that for the period of 1962-66; on the other hand, the number was smaller in the suburbs than that for the period of 1962-66. For the period 1972-76, the number of days with heavy precipitation was larger in the urban area (14) than in the suburbs (8), in contrast to the preceding periods.

Figures 4-2, 4-3, and 4-4 suggest that heavy precipitation has recently come to occur more frequently in the urban area than before. This suggestion is derived from the number of days with classified precipitation at the three stations in the urban area and in the suburbs. Figure 4-5 offers confirmation that the three stations are representative of their areas.

Figure 4-5 shows the same change in the number of days with heavy precipitation as shown in Fig. 4-4. For the periods 1957-61 and 1962-66, the numbers of days with

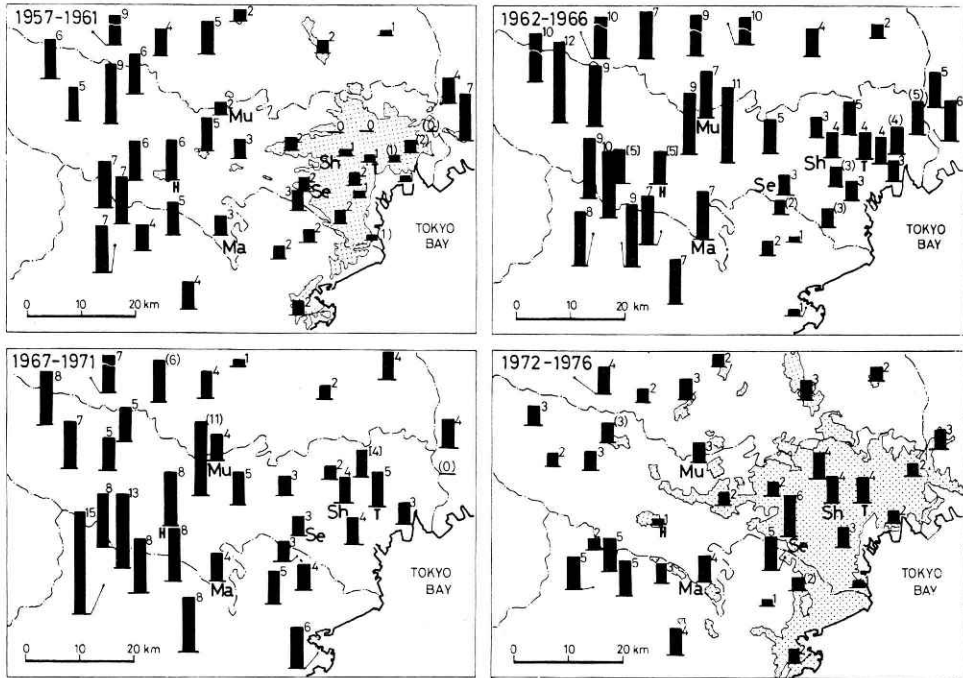


Fig. 4-5 Variation in number of days with heavy precipitation ($\geq 31\text{mm}$) every five years at each station. Dotted areas indicate built-up areas at the indicated time. Parentheses and brackets indicate that data are missing in one year and two years, respectively.

heavy precipitation were smaller in the urban area. The number of days with heavy precipitation increased locally in the urban area for the period 1967-71. For the period 1972-76, the situation was entirely different: the number of days with heavy precipitation was larger in the built-up area than in the surroundings.

Three statistical tests of the differences were made. Data used were the mean values among the number of days with heavy precipitation taken from six stations in the urban center and taken from 14 stations in the surroundings during the period of 1957-66 and the period of 1972-76. The test of multivariate statistical methods indicated that the increase in the number of days with heavy precipitation in the built-up area was significant at the 1% level. The Wilcoxon test and the matched pair t -test indicated a statistical significance at the 5% level.

Temperature differences between the built-up area and surroundings in Tokyo were studied over five years at an interval of five years during the period of 1955-75 (Kawamura, 1977). Two discrete time series of histograms of the differences in maximum and minimum temperatures on a day in summer showed the following: larger temperature differences, say more than 4°C in the daily minimum temperature and more than 2°C in the daily maximum temperature, occurred frequently in 1975, while they occurred only on rare occasions in 1955, 1960, 1965 and 1970. This suggested that a more noticeable urban heat island appeared more often in Tokyo in 1975 than in previous years. It was also after 1970 that the number of days with heavy precipitation became greater in the urban area than in the surroundings.

4-1-4 Situations for the period 1977-86

Figure 4-6 shows the change in the number of days with heavy precipitation in the built-up area and surroundings every five years during the 1977-86 period. The data used are the AMeDAS data as mentioned previously. For both periods of 1977-81 and 1982-86, the situations were different from ones until 1971, but the difference between the number of days with heavy precipitation in the built-up area and in the surroundings are not so large as those for 1972-76.

Figure 4-7 shows maximum temperature differences between the built-up area and surroundings in August in 1977, 1982 and 1987. The temperature difference is the excess of the highest daily maximum temperature among the values at the four AMeDAS stations in the Tokyo built-up area over the lowest daily maximum temperature among the five AMeDAS stations in Tokyo except for the built-up area and Ogochi. The reason why the Ogochi station is excluded is that it is located in a mountainous area more than 60 km from the center of the built-up area and its value is almost always the smallest.

Temperature differences of more than 3°C occurred more often in 1977 than in 1982, and in 1982 than in 1987. The averages of the temperature difference are 2.4°C in 1977, 2.0°C in 1982, and 1.8°C in 1987. The temperature differences between the AMeDAS stations in the built-up area and surroundings become smaller, and this may mean the temperature differences between the built-up area and surroundings has become smaller as a whole. Thus it is suggested that in recent years a remarkable heat island has come to appear less frequently in Tokyo than in the period around 1977.

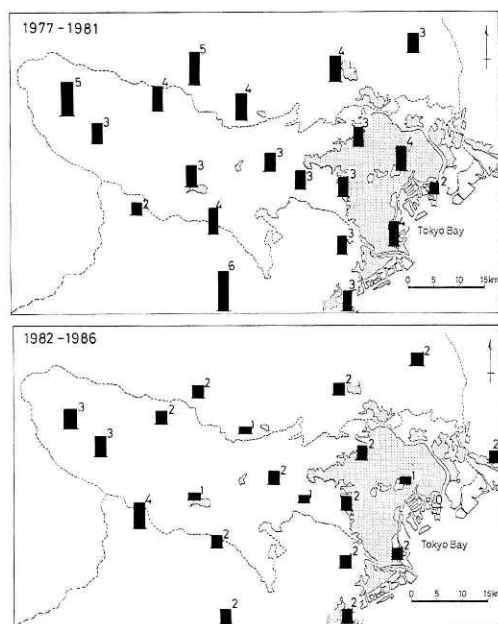


Fig. 4-6 Same as Fig. 4-5 except after 1977.

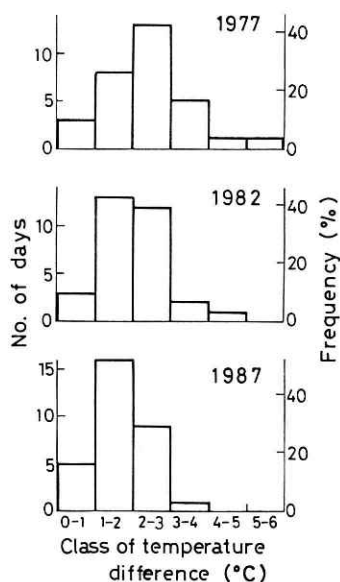


Fig. 4-7 Histograms of excess of maximum temperature in the built-up area over that in the surroundings in August 1977, 1982 and 1987.

The distributions of the number of days with heavy precipitation show that recent trend for the Tokyo built-up area to have more days with heavy precipitation is not as noticeable from the later half of the 1970's. Thus, there was again the coincidence in times between the trends of the frequencies of occurrence of heavy precipitation and higher temperature in the Tokyo built-up area.

4-2 *Possibility for the Heat Island to Affect Precipitation*

All studies previously examined in this paper were made to show the heat island effect on the occurrence of convective precipitation. The purpose of this section is to estimate the possibility for heat island to affect the occurrence of convective precipitation.

4-2-1 Basic assumptions and data used

For the purpose of this section, it is desirable if possible to show the relation between the intensity of the heat island and the excess of rainfall in the built-up area over the amount estimated from atmospheric conditions. But a correct amount of rainfall can not be estimated because there are many factors that affect the amount of rainfall such as stability of atmosphere, wind profile, topography as well as many others. So, the discussion in this section will be made under the following assumptions.

- (a) It was favorable for the occurrence of strong convective precipitation when an hourly precipitation of not less than 10 mm (this is called strong precipitation hereafter) was locally recorded at any AMeDAS point in Tokyo-to.
- (b) The occurrence of strong precipitation in the built-up area was more or less affected by the heat island when it existed about one hour prior to the occurrence of the strong precipitation.

AMeDAS data and data recorded at temperature, wind and humidity stations in the Tokyo-to are used. Since the data of Tokyo-to are available after 1983, studies are made in July and August from 1983 to 1986.

4-2-2 *Conditions on days with strong precipitation in the Tokyo built-up area*

There were eleven days when strong precipitation was locally recorded at AMeDAS points in the Tokyo built-up area. On all days, there were heat islands an hour prior to the occurrence of strong precipitation. On the other hand, there were 20 days with strong precipitation in the surroundings.

Figure 4-8 shows the distributions of the daily mean humidity at the Tokyo Meteorological observatory on days with strong precipitation in the built-up area and in the surroundings. Their average are 84% on days with strong precipitation in the built-up area and 74% on days with strong precipitation in surroundings. The number of days when the mean relative humidity was less than 80% is only two among the 11 days with strong precipitation in the built-up area, while it is 14 for days with strong precipitation in the surroundings; that is 70% of the 20 days. This condition agrees with the fact that urban effects on precipitation are suppressed in dry summers as described previously.

An hour prior to the time when strong precipitation began to rain in the surroundings, there was a heat island in the built-up area in almost every case, although its intensity was different from case to case. Figure 4-9 shows the distributions of the

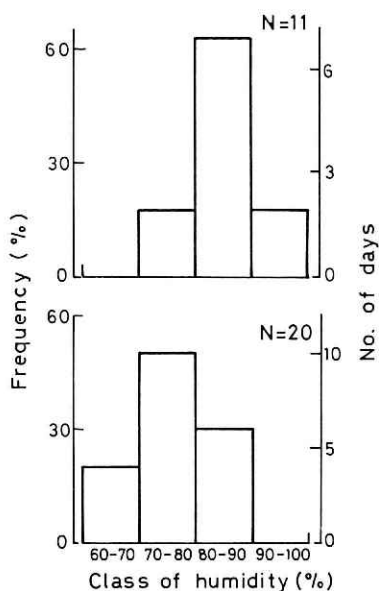


Fig. 4-8 Histograms of daily mean humidity on days with strong precipitation in the Tokyo built-up area (upper) and in the surroundings (lower). N indicstes the total number of events.

surface temperature on days with strong precipitation in the surroundings and a mean humidity of not less than 79%. It is obvious that these heat islands were not so intense as the ones in the cases of 22 July, 1981 and 14 July, 1985 (see Figs. 3-4 and 3-9).

Figure 4-10 shows the distributions of the surface temperature an hour prior to the occurrence of strong precipitation in the Tokyo built-up area on days with a mean humidity of less than 80%. The area where the temperature was higher than in the surroundings by 2°C was noticeable in each case. Among the 6 cases when strong precipitation occurred only in the surroundings and the mean humidity was over 80%, the number of cases where the intense heat island like the one shown in Fig. 4-10 is four at most. Those cases are a, b, c and f. In these four cases, there was no difference in atmospheric conditions and the heat island intensity from situations on days with strong precipitation in the Tokyo built-up area.

On the other hand, there were 62 days with 80% relative humidity and no strong precipitation. Temperature distributions at 15 JST showed that there was a heat island on ten days selected randomly from these days. It may be that there were many days when a heat island did not cause strong precipitation though the mean humidity was over 80%.

Here it should be noted that there were only 15 days when local strong precipitation occurred in the built-up area or in its surroundings among 72 days with 80% relative humidity and 31 days when local strong precipitation occurred among 248 days during July and August in a four year time period. This means that it seldom rains more than 10 mm in an hour. It may be that mechanisms which cause strong precipitation do not work so efficiently in nature.

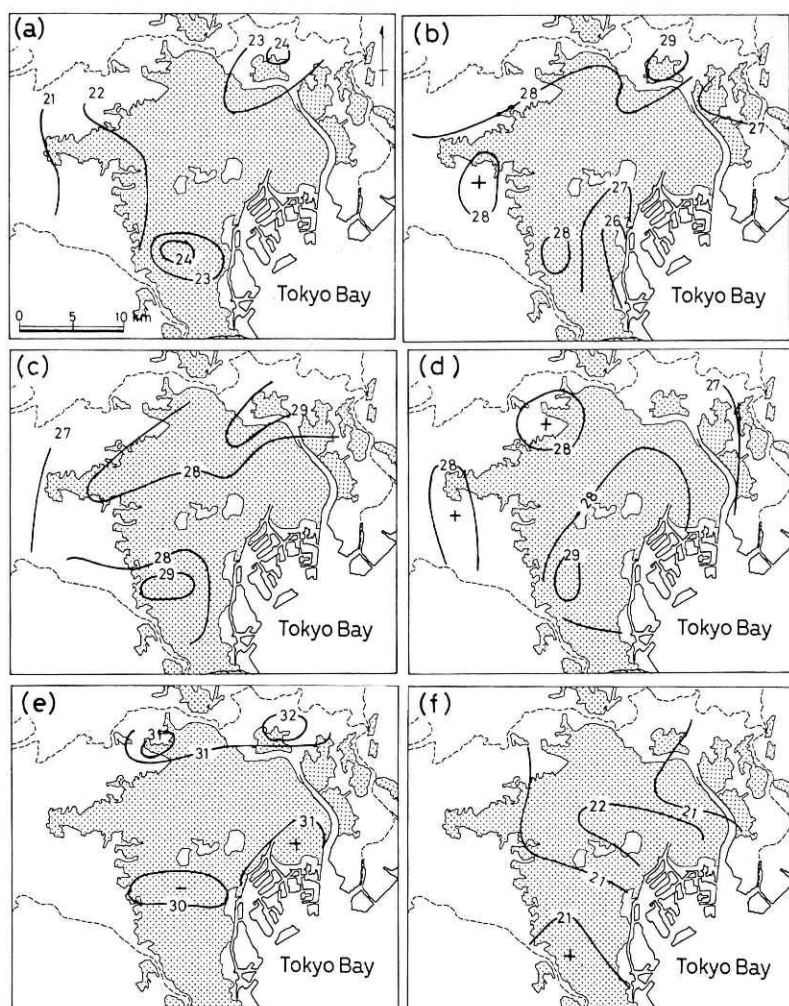


Fig. 4-9 Distribution of surface temperature on days with strong precipitation in the surroundings at an hour before the occurrence of strong precipitation. The dates are ; (a) 7 July, 1984 ; (b) 11 July, 1984 ; (c) 19 July, 1984 ; (d) 12 July, 1985 ; (e) 20 July, 1985 and (f) 1 July, 1986.

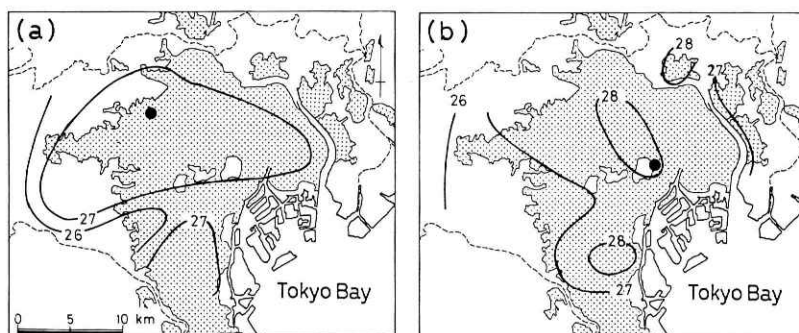


Fig. 4-10 Same as Fig. 4-9 except on days with strong precipitation in the Tokyo built-up area. The dates are : (a) 20 Aug., 1984 and (b) 22 Aug., 1984.

When the mean humidity was over 80%, strong precipitation occurred more often in the built-up area of Tokyo. The number of raingauge stations is 5 in both the built-up area and the surroundings. The average monthly total precipitation is smallest in the area around the Tokyo Bay and largest in the western mountainous areas in the summer. Thus, the larger number of days with strong precipitation in the built-up area rather than in the surroundings suggests that a heat island may cause strong convective precipitation more efficiently than other mechanisms which cause strong convective precipitation.

When humidity was not so high, strong precipitation occurred more often in the surroundings than in the built-up area. This suggests that the ability of a heat island to produce convective precipitation is not high as that of the mechanism in the surrounding.

4-3 Discussion

The following anomalies of daily precipitation in August are presented in the Tokyo built-up area. (a) Heavy precipitation has recently occurred more often in the built-up area. (b) It is suggested that this tendency is not seen in August when it is dry and the monthly totals of precipitation are small. These anomalies agree with those that have been shown in other cities. For example, a high number of days with heavier precipitation has been shown in St. Louis (Changnon et al., 1976) and in Detroit-Windsor (Sanderson and Gorski, 1978). Suppression of urban effects on the amount of precipitation in dry summers has also been shown in the amount of precipitation in St. Louis (Huff and Changnon, 1972).

There is a consistent coincidence between the frequencies of occurrence of the heavy precipitation and the noticeable urban heat island in the Tokyo built-up area. The number of days with heavy precipitation became greater in the built-up area during the period when the noticeable heat island was suggested to appear more often. When the frequency of appearance of the noticeable heat island decreased, the numbers of days with heavy precipitation also decreased to be almost equal to each other in both the built-up area and in its surroundings.

It is shown that the built-up area of Tokyo has recently had a lower temperature excess than in around 1975. Therefore, it might be expected that there would also be a change in population because the urban heat island intensity increases generally with urban population (Oke, 1973; Park, 1987).

Figure 4-11 shows the changes in population in the all "Ku" (center of Tokyo) and the other areas in the Tokyo-to area. The population peaked at 8,893,000 in 1965 and has subsequently fallen in the "ku", while the day population increased till 1975 and decreased after that till 1980. On the other hand, the other areas in the Tokyo area have been gaining population. The population increased by 405,000 at daytime and 445,000 at night from 1975 to 1985.

The changes of the day population of all "ku" and the other areas can not explain the descent in the urban effect on temperature after 1975, because the day population did not remarkably decrease nor increase as is shown in the figure. It, however, is suggested that the trend of urbanization may have changed since about 1975. It is well known that urbanization was encouraged as a national policy from 1972 to 1975 and the whole economic condition of Japan has stabilized after the oil crises of 1973 and 1979. These

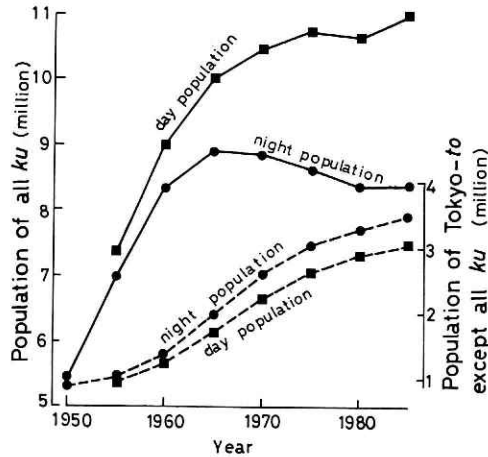


Fig. 4-11 Time variations of populations of all "ku" (solid lines) and those of Tokyo-to except all "ku" (broken lines).

conditions suggest that the temperature in the surroundings has risen through urbanization in the surroundings, and that the temperature difference has become smaller between the Tokyo built-up area and the surroundings.

Here, the results of the theoretical study from Chapter 2 should be noted. The numerical simulations show that a heat island with a larger radius affects the development of convective clouds less when the radius is over 6 km. This could explain the situation in the occurrence of heavy precipitation after the time period around 1977, because it is suggested that the area with higher temperature has become larger after the time period around 1977.

The time changes of these three items, the frequency of occurrence of heavy precipitation in the Tokyo built-up area, that of the intense heat island and the changes of the population of the center of Tokyo and the other areas of the Tokyo-to, present a similar trend. This fact indicates the followings: (1) the increment of the number of days with heavy precipitation in the Tokyo built-up area was caused by the urban effect; and (2) the heat island is a predominant causative factor in the urban enhancement of convective precipitation, as suggested by Pary (1956), Atkinson (1971) and Harnack and Landsberg (1975).

Section 4-2 indicates that a heat island could cause convective precipitation with high probability as compared with the ability of other mechanisms which produce convective precipitation when atmospheric conditions are suitable. Conditions favorable for the occurrence of strong precipitation in the Tokyo built-up area contain high humidity.

Because strong precipitation occurred in the surroundings when humidity was relatively low and the number of days with strong precipitation was larger in the surroundings than in the built-up area, the ability of the heat island to cause convective precipitation is considered not to be so high as that of the mechanisms which produce convective precipitation in the surroundings. Although a heat island is less capable of producing convective precipitation, the heat island effect on precipitation is marked enough to increase the number of days with heavy precipitation in accordance with the

increment of appearance of a noticeable heat island.

5. CONCLUSIONS

Urban effects on the occurrence of convective precipitation are studied from three different approaches: theoretical, case studies, and statistical analysis. Each study shows that a heat island has a marked influence on the development of a convective phenomenon with precipitation.

The numerical experiments show the following. Under conditions that the atmosphere is stable and there is no general wind, (1) a heat island so modifies the atmosphere that atmospheric conditions may be favorable for the development of a convective cloud, (2) a heat island can initiate a cumulus which develops well to cause rain, and (3) there is a size considered suitable for the heat island to cause cumulus convection to be most active; that is an area with a radius of 3-12km which is comparable to the size of a heat island in urban areas. A heat island with a 2°C temperature excess and 6km radius initiates a convective cloud in about 42 minutes. The cloud develops well to cause rain measuring 21mm at the center of the heat island.

It is also shown that it is the upward motion of air induced by the heat island that enhances the activity of a convective cloud. This is because the energy source of convective activity is the latent heat released by condensation of water vapour which is transported from the subcloud layer to a convective cloud.

On 22 July, 1981, many rain gauge stations recorded very heavy rainfall in the Tokyo built-up area. The peak value was 71mm in an hour. The analysis of this case shows what the numerical study presents. Convective clouds formed over a noticeable heat island and they developed well there causing a very heavy rainfall of 79mm. It is also shown that a part of the storm system locally cause heavy rainfall in and in the vicinity of another noticeable heat island. The sizes of these heat islands were comparable to the "suitable" one for a heat island to enhance the convective activity most remarkably, as shown by the numerical simulations. This case gives certain evidence that a heat island could actually aggravate a convective storm.

The analysis of two other cases where the highest hourly rainfall and extremely large hourly rainfall in May were recorded in the built-up area show results that a noticeable heat island existed about an hour prior to the occurrence of heavy rainfall. Heavy rainfall was recorded in and in the vicinity of the heat island in the case of 14 July, 1985 just like the case of 22 July, 1981. In these cases, general wind was very weak in the lower layer. When the general wind was strong, the area that received heavy rainfall was located a little apart from an obvious heat island in the direction of the wind. These features support that the heat island enhanced convective activity to cause heavy rainfall.

The statistical analysis of daily precipitation taken from the month of August shows a recent trend for the Tokyo built-up area to have heavy precipitation more often after 1970. This tendency was most remarkable in the first half of the 1970's. It was also in the first half of the 1970's that an intense heat island appeared most often. This coincidence in period suggests that the heat island is a predominant causative factor in the occurrence of heavy rainfall in the Tokyo built-up area.

Conditions favorable for the occurrence of strong precipitation in the Tokyo built-up area are also studied. The average daily mean relative humidity is 84% on days with strong precipitation, i.e., more than 10mm in an hour, in the built-up area, while it is 74% on days with strong precipitation in the surroundings. This means that the ability of the heat island to cause convective precipitation is not so high as the effects of other mechanisms involved.

Among six days with large precipitation in the surroundings and a mean relative humidity of not less than 80%, there were four days when there was a noticeable heat island in the built-up area. However, there were 11 days with strong precipitation in the built-up area and there were noticeable heat islands on all those days. When relative humidity was over 80%, the number of days with strong precipitation in the built-up area was larger than in the surroundings despite the fact that the total monthly precipitation is larger in the surroundings than in the built-up area in the summer. These findings suggest that a heat island can cause convective precipitation more efficiently than other mechanisms which produce convective precipitation when the atmospheric conditions are favorable.

The following conclusions are drawn from the results of the three different kinds of study contained herein. A noticeable heat island in urban areas can be an important causative factor in the occurrence of convective precipitation, especially in humid areas. This is because the heat island induces an upward motion of air over it. The upward motion can be a triggering force for the occurrence of a convective storm and can enhance convective activity by increasing the amount of water vapour transported to a convective storm.

The results of this paper show that the heat island which urbanization forms so modifies the atmosphere that its conditions may be favorable for the occurrence of convective storms. As described in the introduction, preventive structures against floods are designed using design rainfalls. The design rainfall is estimated from chronological data of heavy rainfall under the assumption that the probability of the occurrence of extremely heavy rainfall is constant in the future. The results of this study claim that planning of counter-measures against floods, such as improvements of rivers and embankments, should take into account the fact that urbanization has increasing effects on the occurrence of heavy rainfall. The results also suggest the possibilities of rain-making by causing upward motion in a lower layer.

ACKNOWLEDGMENTS

The author would like to express his sincere gratitude to Professor M. M. Yoshino of the University of Tsukuba, for his continuing suggestions and encouragement throughout the present study. The author is also grateful to Professors T. Kawamura and T. Nishizawa of the University of Tsukuba for their helpful advice. Frequent and stimulating discussion with Dr. T. Kinoshita of the National Research Center for Disaster Prevention is also gratefully acknowledged.

The author is also deeply indebted to Dr. K. Noda of the Institute of Statistical Mathematics for advice on performing the statistical analyses.

Thanks are also extended to the Japan Meteorological Agency, the Keihin Work

office of the Ministry of Construction, the Tokyo Metropolitan Government, Kanagawa Prefecture and Saitama Prefecture for providing meteorological data.

APPENDIX A

Derivation of Governing Equations of Cumulus Convection

The basic equations used in Chapter 2 are similar to those derived by Ogura and Phillips (1962) for deep moist convection whose order of size is 10km or more. The set of equations in cylindrical coordinates will be presented.

The horizontal and vertical equations of motion are

$$\frac{\partial u}{\partial t} = -u \frac{\partial u}{\partial r} - w \frac{\partial u}{\partial z} - \frac{1}{\bar{\rho}} \frac{\partial P}{\partial r} + F_r, \quad (1)$$

$$\begin{aligned} \frac{\partial w}{\partial t} &= -u \frac{\partial w}{\partial r} - w \frac{\partial w}{\partial z} - \frac{1}{\bar{\rho}} \frac{\partial P}{\partial z} - g + F_z \\ &= -u \frac{\partial w}{\partial r} - w \frac{\partial w}{\partial z} + g \left\{ \frac{T_v - \bar{T}_v}{\bar{T}_v} - Q_t - \frac{P - \bar{P}}{\bar{P}} \right\} - \frac{1}{\bar{\rho}} \frac{\partial (P - \bar{P})}{\partial z} + F_z, \end{aligned} \quad (2)$$

where

$$F_r = \nu \left(\frac{1}{r} \frac{\partial}{\partial r} r \frac{\partial u}{\partial r} + \frac{1}{\bar{\rho}} \frac{\partial}{\partial z} \bar{\rho} \frac{\partial u}{\partial z} - \frac{u}{r^2} \right), \quad (3)$$

$$F_z = \nu \left(\frac{1}{r} \frac{\partial}{\partial r} r \frac{\partial w}{\partial r} + \frac{1}{\bar{\rho}} \frac{\partial}{\partial z} \bar{\rho} \frac{\partial w}{\partial z} \right). \quad (4)$$

The ice phase of water is excluded and two classes of liquid water are considered: cloud droplets and raindrops. The fourth term in the right side of Eq (2) (lower) represents the drag force of raindrops. The equation of mass continuity of air for deep convection is

$$\frac{\partial}{\partial r} (r \bar{\rho} u) + \frac{\partial}{\partial z} (r \bar{\rho} w) = 0. \quad (5)$$

For simplicity in numerical integration, a vorticity equation is introduced. The vorticity is defined as

$$\eta = \frac{\partial \bar{\rho} u}{\partial z} - \frac{\partial \bar{\rho} w}{\partial r}. \quad (6)$$

Cross differentiating Eqs. (1) and (2) yields

$$\begin{aligned} \frac{\partial \eta}{\partial t} &= -u \frac{\partial \eta}{\partial r} - w \frac{\partial \eta}{\partial z} + \left(\frac{2w}{\bar{\rho}} \frac{\partial \bar{\rho}}{\partial z} + \frac{u}{r} \right) \left(\eta - u \frac{\partial \bar{\rho}}{\partial z} \right) + uw \frac{\partial^2 \bar{\rho}}{\partial z^2} \\ &\quad - \bar{\rho} g \frac{\partial}{\partial r} \left(\frac{T_v}{\bar{T}_v} - Q_t \right) + \frac{\bar{\rho} g}{\bar{P}} \frac{\partial P}{\partial r} + D_\eta, \end{aligned} \quad (7)$$

where

$$D_\eta = \nu \left(\frac{1}{r} \frac{\partial}{\partial r} r \frac{\partial \eta}{\partial r} + \frac{1}{\bar{\rho}} \frac{\partial}{\partial z} \bar{\rho} \frac{\partial \eta}{\partial z} - \frac{\eta}{r^2} \right). \quad (8)$$

A streamfunction ψ is defined in relation with u and w as

$$r \bar{\rho} u = \frac{\partial \psi}{\partial z}, \quad r \bar{\rho} w = - \frac{\partial \psi}{\partial r}. \quad (9)$$

Substituting (9) into (6) yields

$$\eta = \frac{1}{r} \frac{\partial^2 \psi}{\partial z^2} + \frac{\partial}{\partial r} \left(\frac{1}{r} \frac{\partial \psi}{\partial r} \right). \quad (10)$$

With the boundary conditions of ϕ , Eq. (10) can be solved for ϕ using the fast Fourier transformation scheme (Ogura, 1969). The wind components u and w can then be determined from (9).

The equation of mass continuity of water substance is

$$\frac{\partial Q_t}{\partial t} = -u \frac{\partial Q_t}{\partial r} - w \frac{\partial Q_t}{\partial z} + \frac{1}{\bar{\rho}} \frac{\partial}{\partial z} (\bar{\rho} V_r Q_r) + D(Q_v + Q_c). \quad (11)$$

In Eqs. (11) and (13) below, the assumption has been made that the cloud droplets have negligible terminal velocity and therefore always follow the air flow. A raindrop falls at a representative terminal velocity relative to the air flow. The third term on the right-hand side of Eq. (11) accounts for the redistribution of rainwater as it falls.

The equations for air temperature and water vapour are closely related. In the unsaturated region, the equations are

$$\frac{\partial T}{\partial t} = -u \frac{\partial T}{\partial r} - w \left(\frac{\partial T}{\partial z} + \Gamma_d \right) - \frac{L_e}{c_p} P_e + D_T, \quad (12)$$

$$\frac{\partial Q_v}{\partial t} = -u \frac{\partial Q_v}{\partial r} - w \frac{\partial Q_v}{\partial z} + P_e + D_{Q_v}, \quad (13)$$

where term P_e represents the rate of evaporation of cloud droplets or raindrops. Cloud droplets are assumed to evaporate instantly if the air is not saturated. The rate of evaporation is determined so as to keep the air at the saturation level until the cloud droplets are totally evaporated. The raindrops will evaporate only if the cloud droplets are exhausted. The evaporation rate of raindrops is in proportion to the saturation deficit at a constant rate of 10^{-3} /s following Yoshizaki (1978).

In the saturated region

$$\frac{\partial T}{\partial t} = \left\{ -u \frac{\partial T}{\partial r} - w \left(\frac{\partial T}{\partial z} + \Gamma_d \right) + \frac{L_e}{c_p} \left(-u \frac{\partial Q_v}{\partial r} - w \frac{\partial Q_v}{\partial z} + D_{Q_v} \right) + D_T \right\} / \left(1 + \frac{L_e^2 q_s}{c_p R_v T^2} \right), \quad (14)$$

$$\frac{\partial Q_v}{\partial t} = \frac{\partial q_s}{\partial t}, \quad (15)$$

$$\frac{\partial Q_c}{\partial t} = -u \frac{\partial Q_c}{\partial r} - w \frac{\partial Q_c}{\partial z} + P_c - P_r + D_{Q_c}. \quad (16)$$

The term P_c in Eq. (16) represents the rate of condensation which takes place whenever air is supersaturated or the rate of evaporation which takes place whenever air is unsaturated until the air is saturated. The term P_r represents the rates of production of rainwater through processes of auto-conversion and collection. These rates are represented by Kessler's (1969) formula, i. e. Eq. (17), with the parameters $k_1 = 0$ for $Q_c \leq 10^{-3}$ and $k_1 = 10^{-3}$ for $Q_c > 10^{-3}$ gm gm $^{-1}$ after Soong and Ogura (1973).

$$P_r = k_1 (Q_c - 10^{-3}) + 2.2 Q_c \cdot Q_r^{0.875}. \quad (17)$$

APPENDIX B

Amount(mm) of precipitation on days when a typhoon or a tropical depression affected the weather in Tokyo in August.

Year	August date	Distur- bance	Tokyo	Shinjuku	Setagaya	Murayama	Hachioji	Machida
1958	23	Ty 17	27	25	4	15	55	48
	24		9	11	10	22	50	15
	25		15	22	27	42	49	40
1959	8	Ty 6	11	26	19	44	98	42
	9		24	26	47	33	32	24
	12	Ty 7	45	39	25	53	98	46
	13		21	31	53	74	89	62
1960	19	Ty 14	48	53	57	57	69	47
	20		53	46	59	53	43	33
1963	28	Ty 11	155	152	154	87	158	139
1964	20	De	78	73	58	97	144	98
1965	21	Ty 17	96	108	80	90	missing missing	120
	22		83	79	64	75		76
1969	4	Ty 7	45	25	18	30	17	53
	23	Ty 9	32	36	42	22	35	17
1971	30	Ty 23	93	67	95	130	177	133
	31		88	78	35	42	20	29
1972	7	Ty 13	14	26	19	38	28	19
1974	24	Ty 14	5	5	5	27	59	13
	25		37	43	50	105	117	57
	31	Ty 16	79	80	53	105	153	80
1975	22	Ty 6	1	2	4	30	86	45
	23		2	—	6	13	25	5

The disturbance symbols are: Ty, typhoon; De, tropical depression.

REFERENCES

- Asai, T., 1964: Cumulus convection in the atmosphere with vertical wind shear: Numerical experiment. *J. Meteor. Soc. Japan*, **42**, 245-259.
- Asai, T., 1967: On the characteristics of cellur cumulus convection. *J. Meteor. Soc. Japan*, **45**, 251-260.
- Ashworth, J. R., 1929: The influence of smoke and hot gases from factory chimneys on rainfall. *Quart. J. Royal Meteorol. Soc.*, **55**, 341-350.
- Atkinson, B. W., 1971: The effect of an urban area on the precipitation from a moving thunderstorm. *J. Appl. Meteor.*, **10**, 47-55.
- Bornstein, R.D., 1968: Observations of the urban heat island effect in New York City. *J. Appl. Meteor.*, **7**, 575-582.
- Braham, R. R., Jr., and M. J. Dungey, 1978: A study of urban effects on radar first echoes. *J. Appl. Meteor.*, **17**, 644-654.
- Braham, R. R., Jr., and D. Wilson, 1978: Effects of St. Louis on convective cloud heights. *J. Appl. Meteor.*, **17**, 587-592.
- Byers, H. R., and R. R. Braham, 1949: *The thunderstorm*. U. S. Govt. Printing Office, Washington D. C., 287pp.
- Carrea, G., 1975: Rainfall of Thursdays. *Weather*, **30**, 168.
- Chandler, T. J., 1965: *The climate of London*. Hutchinson, London, 292pp.
- Chandler, T. J., 1970: Urban climatology: Summary and conclusion of the symposium. *WMO Techn. Notes*, **108**, 375-377.
- Changnon, S. A. Jr., 1968: The La Porte weather anomaly—fact or fiction? *Bull. Amer. Meteor. Soc.*, **49**, 4-11.
- Changnon, S. A. Jr., 1970: Reply (to Holtzman and Thom). *Bull. Amer. Meteor. Soc.*, **51**, 337-342.
- Changnon, S. A. Jr., 1971: Comments on "The effect on rainfall of a large steelworks". *J. Appl. Meteor.*, **10**, 165-167.
- Changnon, S. A. Jr., 1978: Urban effects on severe local storms at St. Louis. *J. Appl. Meteor.*, **17**, 578-586.
- Changnon, S. A. Jr., R. G. Semonin, and F. A. Huff, 1976: A hypothesis for urban rainfall anomalies. *J. Appl. Meteor.*, **15**, 544-560.
- Charton, F. L., and J. R. Harman, 1973: An additional comment on the La Porte precipitation anomaly. *Bull. Amer. Meteor. Soc.*, **54**, 26.
- Daigo, Y. and T. Nagao, 1972: *Toshikikougaku*, Asakura Shoten, Tokyo, 214pp (in Japanese).
- Delage, Y., and P. A. Taylor, 1970: Numerical studies of heat island circulations. *Boundary-Layer Meteor.*, **1**, 201-226.
- Dettwiller, J., 1970: Incidence possible de l'activite industrielle sur les precipitations a Paris. In *Urban Climates, Technical Note No. 18*, World Meteorological Organization, Geneva, 361-362.
- Dettwiller, J., and S. A. Changnon, 1976: Possible urban effects on maximum daily rainfall at Paris, St. Louis and Chicago. *J. Appl. Meteor.*, **15**, 517-519.
- Duckworth, F. S., and J. S. Sandberg, 1954: The effect of cities upon horizontal and vertical temperature gradients. *Bull. Amer. Meteor. Soc.*, **35**, 198-207.
- Elliott, W. P., and F. L. Ramsey, 1970: Comments on "Cloud condensation nuclei from industrial sources and their apparent influence on precipitation in Washington State". *J. Atmos. Sci.*,

- 27, 1215-1216.
- Fritts, H. C., and W. C. Ashby, 1973 : Reply (to Charton and Harman). *Bull. Amer. Meteor. Soc.*, **54**, 26-27.
- Fukui, E. and G. Koizumi, 1938 : Dai Tokyo niokeru uryo no bunpu. *Geo. Rev. Japan*, **14**, 465-487 (in Japanese).
- Garstang, M., P. D. Tyson, and G. D. Emmitt, 1975 : The structure of heat islands. *Reviews of Geophysics and Spacephysics*, **13**, 139-165.
- Harman, J. R., and W. M. Elton, 1971 : The La Porte, Indiana, precipitation anomaly. *Ann. Assoc. Amer. Geogra.*, **61**, 468-480.
- Harnack, R. P., and H. E. Landsberg, 1975 : Selected cases of convective precipitation caused by the metropolitan area of Washington, D. C. *J. Appl. Meteor.*, **14**, 1050-1060.
- Hidore, J. J., 1971 : The effects of accidental weather modification on flow of Kankakee River. *Bull. Amer. Meteor. Soc.*, **52**, 99-103.
- Hill, G. E., 1974 : Factors controlling the size and spacing of cumulus clouds as revealed by numerical experiments. *J. Atmos. Sci.*, **31**, 646-673.
- Hindman, E. E., II, P. M. Tag, B. A. Silberman, and P. V. Hobbs, 1977 : Cloud condensation nuclei from a paper mill. Part II ; Calculated effects on rainfall. *J. Appl. Meteor.*, **16**, 753-755.
- Hobbs, P. V., L. F. Radke, and S. E. Shumway, 1970a : Cloud condensation nuclei from industrial sources and their apparent influence on precipitation in Washington State. *J. Atmos. Sci.*, **27**, 81-89.
- Hobbs, P. V., L. F. Radke, and S. E. Shumway, 1970b : Reply (to Elliott and Ramsey). *J. Atmos. Sci.*, **27**, 1216-1217.
- Holzman, B. G., 1971a : La Porte precipitation fallacy. *Science*, **171**, 847.
- Holzman, B. G., 1971b : More on the La Porte fallacy. *Bull. Amer. Meteor. Soc.*, **52**, 572-574.
- Holzman, B. G., and H. C. S. Thom, 1970 : The La Porte precipitation anomaly. *Bull. Amer. Meteor. Soc.*, **51**, 335-337.
- Huff, F. A., and S. A. Changnon, Jr., 1972 : Climatological assessment of urban effects on precipitation at St. Louis. *J. Appl. Meteor.*, **11**, 823-842.
- Huff, F. A., and S. A. Changnon, Jr., 1973 : Precipitation modification by major urban areas. *Bull. Amer. Meteor. Soc.*, **54**, 1220-1232.
- Kawamura, T., 1964 : Some considerations on the cause of city temperature at Kumagaya city. *Geog. Rev. Japan*, **37**, 243-254.
- Kawamura, T., 1977 : Toshikikou no bunpu no jittai. *Kisho Kenkyu Note*, **133**, 26-47 (in Japanese).
- Kessler, E., 1969 : On the distribution and continuity of water substance in atmospheric circulation. *Meteor. Monogr.*, **10**, No. 32, 84pp.
- Khemani, L. T., and B. V. R. Murty, 1973 : Rainfall variations in an urban industrial region. *J. Appl. Meteor.*, **12**, 187-194.
- Kratzer, A., 1937 : *Das stadtklima*. 1 Aufl. Friedr. Viewg, Braunschweig, 144pp.
- Kuo, H. L., 1963 : Perturbations of plane Couette flow in stratified fluid and origin of cloud streets. *Phys. Fluids*, **6**, 195-211.
- Landsberg, H. E., 1981 : *The urban climate*. Academic Press, New York, 275pp.
- Lawrence, E. N., 1971 : Urban climate and day of the week. *Atmos. Environ.*, **5**, 935-948.
- Lowry, W. P., and F. Probal, 1978 : An attempt to detect the effects of a steelworks on

- precipitation amounts in Central Hungary. *J. Appl. Meteor.*, **17**, 964-975.
- Namias, J., 1966: A weekly periodicity in eastern U. S. precipitation and its relation to hemispheric circulation. *Tellus*, **18**, 731-744.
- Nicholson, G., 1969: Wet Thursdays. *Weather*, **24**, 117-119.
- Norgate, T. B., 1974: Rainfall on Thursdays. *Weather*, **29**, 197.
- Ochs, H. T., 1975: Modeling of cumulus initiation in METROMEX. *J. Appl. Meteor.*, **14**, 873-882.
- Ochs, H. T., and D. B. Johnson, 1980: Urban effects on the properties of radar first echoes. *J. Appl. Meteor.*, **19**, 1160-1166.
- Ochs, H. T., and R. G. Semonin, 1979: Sensitivity of a cloud microphysical model to an urban environment. *J. Appl. Meteor.*, **18**, 1118-1129.
- Ogden, T. L., 1969: The effect of a large steelworks on rainfall. *J. Appl. Meteor.*, **8**, 585-591.
- Ogden, T. L., 1971: Reply (to Changnon). *J. Appl. Meteor.*, **10**, 168.
- Ogura, M., 1969: A direct solution of Poisson's equation by dimension reduction method. *J. Meteor. Soc. Japan*, **47**, 319-323.
- Ogura, Y., and N. A. Phillips, 1962: Scale analysis of deep and shallow convection in the atmosphere. *J. Atmos. Sci.*, **19**, 173-179.
- Oke, T. R., 1973: City size and the urban heat island. *Atmos. Environ.*, **7**, 769-779.
- Park, H. S., 1987: City size and urban heat island intensity for Japanese and Korean cities. *Geog. Rev. Japan (Ser. A)*, **4**, 238-250 (in Japanese with English abstract).
- Parry, M., 1956: An urban rainstorm in the Reading area. *Weather*, **11**, 41-48.
- Petterssen, S., 1956: *Weather Analysis and Forecasting*. vol. II, McGraw-Hill, New-York, 266pp.
- Pittock, A. B., 1977: On the causes of local climatic anomalies, with special reference to precipitation in Washington State. *J. Appl. Meteor.*, **16**, 223-230.
- Sanderson, M., and R. Gorski, 1978: The effect of metropolitan Detroit-Windsor on precipitation. *J. Appl. Meteor.*, **17**, 423-427.
- Sanderson, M., I. Kumanan, T. Tangury, and W. Schertzer, 1973: Three aspects of the urban climate of Detroit-Windsor. *J. Appl. Meteor.*, **12**, 629-638.
- Sawai, T., 1978: Formation of the urban air mass and the associated local circulation. *J. Meteor. Soc. Japan*, **56**, 159-174.
- Schickedanz, P. T., 1974: Inadvertent rain modification as indicated by surface raincells. *J. Appl. Meteor.*, **13**, 891-900.
- Schmauss, A., 1927: Grosstädte und Niederschlag. *Meteor. Z.*, **44**, 339-341.
- Sekiguti, T., 1960: The geographical distribution of spring-time city temperatures in and around Yonezawa, Yamagata, in northern Japan. *Tokyo Geog. Papers*, **4**, 17-40.
- Sekiguti, T., 1970: Toshikikougaku. *Tenki*, **17**, 89-96 (in Japanese).
- Sharon, D., and Koplowitz, R., 1972: Observations of the heat island of a small town. *Met. Rdsch.*, **25**, 143-146.
- Soong, S., and Y. Ogura, 1973: A comparison between axisymmetric and slab-symmetric cumulus cloud models. *J. Atmos. Sci.*, **30**, 879-893.
- Spar, J., and P. Ronberg, 1968: Note on an apparent trend in annual precipitation at New York City. *Monthly Weather Rev.*, **96**, 169-171.
- Squires, P., and K. S. Turner, 1962: An entraining jet model for cumulo-nimbus updraughts. *Tellus*, **14**, 422-434.

- Srivastava, R. C., 1967 : A study of the effect of precipitation on cumulus dynamics. *J. Atmos. Sci.*, **24**, 36-45.
- Sulakvelidze, G. K., 1969 : *Rainstorms and Hail*. Israel Program for Scientific Translations. 310pp.
- Sundborg, Å., 1950 : Local climatological studies of the temprature conditions in an urban area. *Tellus*, **2**, 222-232.
- Warner, J., 1968 : A reduction in rainfall associated with smoke from sugar-cane fires—an inadvertent weather modification? *J. Appl. Meteor.*, **7**, 247-251.
- Yoshino, M. M., 1957 : The distribution of rainfall and the increase of drizzle days in Tokyo. *Tenki*, the 75th anniversary volume., 121-125 (in Japanese).
- Yoshino, M. M., 1975 : *Climate in a small area*. Univ. of Tokyo Press, Tokyo, 549pp.
- Yoshino, M.M., 1977 : Nippon oyobi gaikoku no shotoshi ni okeru kiko no henka. *Kisho Kenkyu Note*, **133**, 1-25 (in Japanese).
- Yoshizaki, M., 1978 : Numerical experiments of a convective cloud with a high cloud base in shear flows. *J. Meteor. Soc. Japan*, **56**, 387-404.

(Manuscript Received July 3, 1989)

Study of the urban effects on the occurrence of convective precipitation

対流性降雨の発生に及ぼす都市の影響に関する研究

米谷恒春

国立防災科学技術センター

要 旨

都市は、エネルギー消費が著しく多いこと、地表面の広い部分がコンクリートなどの無機物に覆われていること等の特徴を有している。このような特異性が大気現象に影響を及ぼし、都市の気候は周辺部と異なる状態を呈している。その代表的なものは都市域で気温が周辺部より高いことであり、ヒートアイランド現象として良く知られている。

本研究は、現象の水平スケールが都市と同程度である対流現象がもたらす降水について、その発生に及ぼすヒートアイランドの影響を調べたものである。下の1～4に記したように、理論的解析、事例解析、及び統計的解析を行い、湿潤地域にある都市では対流性降雨の発生にヒートアイランドが大きな影響を及ぼす、という結論を得た。

1. 理論的解析

ヒートアイランドが存在した場合に大気がどのように変質し、それが対流雲の発生・発達にどのような影響を及ぼすか、及び影響の強さとヒートアイランドの水平規模との関係を数値シミュレーションの方法及び解析の方法により調べた。用いた数値モデルの方程式系は、対流雲の研究等に使用されている一般的なものであり、流体の運動方程式、空気、水の連続の式、及び熱力学の式からなる。

得られた結果は次のようにまとめられる。

- (1) 雲の初期じょう乱が発達し得ない大気状態であっても、中心で気温が周囲より 1.2°C 高いヒートアイランドがあれば、雲の初期じょう乱は良く発達し、降雨が生じた。
- (2) 中心での気温が周囲より 2°C だけ高いヒートアイランドは、その上空に雲を形成した。雲が最も良く発達した場合は、半径が 6 km のときでヒートアイランドの中心に 20 mm を超す雨が降った。
- (3) ヒートアイランドの半径が小さいと雲は早く形成されるが、発達の程度は悪かった。一方、半径が大きすぎると雲を形成するまでに長時間を要し、雲の発達の程度も悪くなった。例えば、半径が 18 km のときは、雲が形成されるまでに 118 分を要し、地上で雨は記録されなかった。
- (4) ヒートアイランドが存在すると対流雲が良く発達するのは、ヒートアイランドに伴う局地循環が、対流活動のエネルギー源となる水蒸気の補給を促すためである。
- (5) ヒートアイランドの半径が小さくても、また大きすぎても、対流活動に及ぼす影響が弱くなるのは次の理由による。半径が小さいと周囲から流入する空気がヒートアイランド上空の気温を短時間のうちに低下させる。一方半径が大きくなると、補償流としての水平流の形成にエネルギーがより多く消費され、上昇流の速さは小さくなる。どちらも対流活動を抑制するように作用する事柄であり、このため、対流活動に最も強い影響を及ぼす半径が存在することになる。

以上の結果は、ある程度の広さと強さを持つヒートアイランドは対流性降雨の発生を促し

たり、その活動の活発化をもたらす能力があることを示している。また、対流活動に顕著な影響を及ぼすヒートアイランドの半径は3～12 km程度であることが示された。この水平規模は現実の都市の水平規模と同程度である。

2. 事例解析

ヒートアイランドが現実に対流性降雨を引き起こしたり、その活動の活発化をもたらしていることを、東京に非常に強い局地的な雨が発生した場合について示した。

1981年7月22日、東京の都心部は集中豪雨に見舞われ、1時間に60 mm以上の雨量を記録した所もあった。東京都が密に展開している気温・風の観測点の記録により地上気温と風の分布を調べたところ、豪雨に襲われた場所は、その発生に先立って高温域となっており、地上風の収束が生じていた。高温域は2ヵ所に存在しており、どちらも中心部の広さは3 km×15 kmで近似できるものであった。

また、東京管区气象台で観測したレーダー記録の解析から、ヒートアイランドの上空で雲が形成されたこと、及び雲は豪雨域よりもはるかに広い領域をおおっていたが、40 mmを超すような豪雨が降った場所はヒートアイランドが存在していた場所とその近傍だけであったことが分かった。

さらに、1985年7月14日及び1979年5月15日の局地的豪雨について、地上気温と風の分布を調べたところ、どちらの場合も上記の例と同様に、地上風の収束を伴う高温域が豪雨の発生に先立って形成されていた。

以上より、ヒートアイランドが対流性降雨を引き起こしたり、その活動をより活発にしていることが、現実が生じていると考えられる。

3. 統計的解析

ヒートアイランドが対流性降雨を引き起こしたり、活発化をもたらすことが例外的現象でないことを、東京の都心部を対象として(1)局地的な大雨が降った日数の経年変化および(2)局地的な強い雨が降った日の気象状態と発生頻度、を検討することにより示した。

- (1) 対流性降雨の発生しやすい8月の局地的な大雨(日降水量が31 mm以上に達した雨)が降った日数について、1954年以降の変化を東京の都心部とその周辺部とで比較した。その結果、1970年代にはいると、それまでの傾向と逆転して都心部で大雨日数が多くなっており、その後、1970年代の後半からは都心部と周辺部とで差が生じていないことが認められた。

都市部と周辺部との気温差は、1975年頃まではその差が大きくなるように変化したことがすでに調べられており、また、1970年代後半以降では、その差が小さくなるように変化した。すなわち、顕著なヒートアイランドの発生頻度が、1975年頃までは年とともに増加したが、その後は減少したと判断される。

都心部における大雨の発生頻度の変化傾向と顕著なヒートアイランドの発生頻度の変化傾向が一致したことから、都心部における局地的な大雨の発生にヒートアイランドが大きく関与している、と考えられる。

- (2) 1983年から1986年までの4年間の7月と8月の、都心部に時間雨量10 mm以上の局地的な強い雨が降った日と周辺部にのみ時間雨量10 mm以上の局地的な強い雨が降った日について、気象状態等を比較し、都心部に強い雨が降った日の特徴として次の事項を得た。
 - ① 都心部に強い雨が降った日は湿度が高かった。都心部に強い雨が降った日、11日のうち9日間は東京管区气象台の平均相対湿度が80%以上であった。一方、周辺部にのみ強い雨が降った日、20日のうち湿度が80%以上であったのは6日にすぎなかった。
 - ② 都心部に強い雨が降ったときは全て、その発生に先立って明瞭なヒートアイランドが

形成されていた。平均湿度が80%以上あって周辺部にのみ強い雨が降った日、6日のうち、都心部に顕著なヒートアイランドが形成されていたのは4日であった。

上記調査での観測点の数は都心部と周辺部とで同じであり、また、7月、8月の月降水量は都心部の方が少ない。この事実にもかかわらず、湿度が高い場合には強い雨が降った日数は都心部で多かった。このことから、条件さえ整えばヒートアイランドが対流性の強い雨を引き起こす確率は、対流性降雨を引き起こす他の機構のものより高いと判断される。一方、周辺部では湿度がそれほど高くない状態のときでも強い雨が降っていることから、ヒートアイランドが対流性降雨をもたらす能力は、周辺部に対流性降雨をもたらす機構の能力ほどには強くないと考えられる。

以上より、ヒートアイランドが対流性降雨に影響を及ぼす能力は周辺部で対流性降雨をもたらす機構のものほど強くはないが、東京ではヒートアイランドが対流性降雨の発生に関与している程度は高く、都心部に対流性降雨をもたらす重要な要因の一つである、と考えられる。

4. 結 論

以上の結果より次の結論を得た。

- (1) 顕著なヒートアイランドは対流性降雨の発生及び対流活動の活発化をもたらす能力がある。
- (2) その能力は対流性降雨を引き起こす他の機構に比して決して高いものではないが、大気条件さえ整えばヒートアイランドは大きい確率で、対流性降雨の発生・活発化をもたらしていることが、東京で生じている。
- (3) 湿潤な地域における都市では、ヒートアイランドは集中豪雨を含む対流性降雨を引き起こす要因となり得る。